Available online at www.sciencedirect.com
SCIENCE DIRECT
J. Vis. Commun. Image R. 17 (2006) 1–26
JOURNAL OF VISUAL Communication & IMAGE Representation
www.elsevier.com/locate/jvci

Vector sigma filters for noise detection and removal in color images

Rastislav Lukac [a,*,1], Bogdan Smolka [b], Konstantinos N. Plataniotis [a], Anastasios N. Venetsanopoulos [a]

[a] *Multimedia Laboratory, The Edward S. Rogers Sr. Department of Electrical and Computer Engineering, University of Toronto, 10 King's College Road, Toronto Ont., Canada M5S 3G4*
[b] *Department of Automatic Control, Silesian University of Technology, Akademicka 16 Str., 44-101 Gliwice, Poland*

Received 25 May 2003; accepted 10 August 2005
Available online 15 November 2005

Abstract

This paper presents a new adaptive filtering approach capable of detecting and removing impulsive noise in multichannel images. The proposed methodology constitutes a powerful unified framework for multichannel signal processing. Robust order-statistic concepts and statistical measure of vectors' deviation are used in conjunction with different distance measures among multichannel inputs to determine an efficient switching rule between filter output and no filtering (identity operation). The special case of color image filtering is studied as an important example of multichannel signal processing. Simulation studies reported in this paper indicate that the proposed filter class is computationally attractive, has excellent performance, and is able to preserve fine details while suppressing impulsive noise.

Keywords: Multichannel image processing; Nonlinear vector filtering; Order-statistic theory; Adaptive filter design

1. Introduction

The perception of color is of paramount importance to humans and automatic vision systems, since they use color information to sense the environment and recognize the objects on the scene [1]. Because the acquisition or transmission of digital images through sensors or communication channels is often inferred by impulsive noise [1–4] (e.g., bit errors [5] or mixed impulsive and Gaussian noise [2,5]), the aim of pre-processing techniques is the noise filtering [1,2,5,6,7] which enables communication in noisy environments [5] and processing of different kinds of multichannel images (e.g., enhancement of cDNA microarray images [8,9], digitized artwork images [10,11], old movies [12–14], and images acquired by sensors [15,16]).

* Corresponding author. Fax: +14 16 978 4425.
E-mail address: lukacr@dsp.utoronto.ca (R. Lukac).
URL: www.dsp.utoronto.ca/~lukacr (R. Lukac).
[1] Partially supported by the NATO/NSERC Science Award.

1047-3203/$ - see front matter © 2005 Elsevier Inc. All rights reserved.
doi:10.1016/j.jvcir.2005.08.007

The goal of the image filtering is the removal of unprofitable information such as various signal distortions in order to obtain the image which corresponds as closely as possible to the output of an ideal imaging system [1]. In many applications, it is indispensable to remove the corrupted pixels to facilitate subsequent image processing operations such as edge detection, image segmentation, and pattern recognition. To convey the desired information correctly, the noisy signal should be processed by a filtering algorithm which removes the noise component, but retains the image structure.

Many of the techniques used for color noise reduction such as componentwise (marginal) median filters [17,18] are direct extensions of the methods used for gray-scale imaging. The independent processing of color image channels is, however, inappropriate and leads to strong color artifacts (sub-optimal estimates in sense of color information), which are caused by scalar ordering of the multichannel samples in the input of the filter. To overcome this problem and avoid the color artifacts produced by marginal approaches, the vector processing of color image data as vector fields is desirable due to the strong correlation that exists among the image channels [1,2,19–22]. Therefore, the standard techniques developed for monochrome images have to be extended in a way which exploits the correlation among the image channels and processes the input multichannel samples as the set of image vectors.

If the noise corrupted image is of impulsive nature (e.g., bit errors and outliers[2]), filtering approaches based on the order-statistics theory are often employed [5,7,23,24]. These nonlinear filters: (i) operate by ordering the image samples inside a processing window, (ii) are able to match the underlying statistical model, and (iii) they are computationally simple. In gray-scale images, the ordering of the samples inside the filter window moves the atypical image samples, often corrupted by noise, to the borders of the ordered set. Therefore, the middle-positioned samples in the ordered sequence represent the robust estimates in the environments corrupted by outliers.

It has been widely recognized [1,2,19–22] that the nonlinear vector processing of color images is the most effective way to filter out outliers. For that reason, a number of filtering approaches, such as those presented in [25–27], have been developed to extend the filtering efficiency of the standard filtering approaches. Vector median filter [19] is a typical example of such an extension, when the median defined over the gray-scale samples has been replaced with the lowest ranked multichannel sample achieved by vector ordering [1]. This filter is very often used for the removal of impulsive noise in color images. On the other hand, the standard median filter [23] or its multichannel extensions, i.e., the vector median filter [19] and the basic vector directional filter [21], are unable to adapt their behavior to varying noise and signal statistics related to the local image information of the samples inside a sliding filtering window. These filters perform the fixed amount of smoothing that results in blurring of fine image details.

The restriction of the filtering to noisy samples only, whereas the desired information is invariant to the filter action, is the subject of this paper. It is focused on an adaptive switching between robust smoothing expressed by the lowest ranked multichannel sample and no filtering (identity operation). The filtering framework developed in the paper is controlled by a comparison of the statistics related to the central input sample and approximation of the variance related to the input set of vectors in the processing window. The proposed methods are simpler than recently developed approaches which extend the design framework of standard filtering schemes by considering weighting coefficients [25–27], sub-window structures [28,29], and similarities of the samples along digital paths [30]. In addition to other approaches [31–35] based on the switching concept, the proposed framework is designed to perform simple, fast, and pure vector operations respecting the nature of color images and computational requirements.

The rest of this paper is organized as follows. In Section 2, a brief overview of the vector ordering and robust order-statistics applied to color images is presented. This section also reviews multichannel filtering schemes widely used to enhance color images. In Section 3, we propose multichannel sigma filter class controlled by the tuning parameter, as well as their fully adaptive multichannel modifications. Motivation and design characteristics of the proposed framework are discussed in detail and modifications of the proposed structure are introduced and analyzed with respect to their properties and used parameters. In Section 4, the proposed method is tested using a wide range of test images and impulsive noise intensities. Finally, this paper concludes in Section 5.

[2] Isolated image samples with a significantly different intensity from the local image neighborhood.

```
Inputs:  NumberOfRows × NumberOfColumns noisy image
         Window size N
         Moving window spawning the input set {x_1, x_2, ..., x_N}
Output:  NumberOfRows × NumberOfColumns image

For a = 1 to NumberOfRows
  For b = 1 to NumberOfColumns
    Determine the input set W(a,b) = {x_1, x_2, ..., x_N}
    For i = 1 to N
      For j = 1 to N
        Compute the distance f(x_i, x_j)
      end
      Compute the sum ξ_i = f(x_i, x_1) + f(x_i, x_2) + ... + f(x_i, x_N)
    end
    Sort ξ_1, ξ_2, ..., ξ_N to the ordered set ξ_(1) ≤ ξ_(2) ≤ ... ≤ ξ_(N)
    Apply the same ordering to x_1(ξ_1), x_2(ξ_2), ..., x_N(ξ_N)
    Store ordered sequence as x_(1) ≤ x_(2) ≤ ... ≤ x_(N)
    Let the filter output y(a,b) = x_(1)
  End
End
```

Fig. 1. Algorithm of the vector filters outputting the lowest ranked vector according to a specific ordering technique.

2. Order-statistics in color images

Let $\mathbf{x} : Z^l \rightarrow Z^m$ represent a multichannel image, where l is an image dimension and m denotes the number of channels.[3] Since natural images are nonstationary, filtering schemes operate on the premise that an image can be subdivided into small regions, each of which can be treated as stationary [1]. Using the sliding filter window $W = \{\mathbf{x}_i = (x_{i1}, x_{i2}, \ldots, x_{im}) \in Z^l;\ i = 1, 2, \ldots, N\}$, with x_{ik} for $k = 1, 2, \ldots, m$ denoting the kth element of the vectorial sample $\mathbf{x}_i$, the procedure replaces the central sample $\mathbf{x}_{(N+1)/2}$ determining the position of the window with the output $\mathbf{y} = \phi(W)$ of a filter function $\phi(\cdot)$ operating over noise corrupted samples listed in W. Thus, the value of the estimated pixel depends on the values of image samples $\mathbf{x}_i$ in its neighborhood.

The most popular color image filters are those based on the concept of robust vector order-statistics (Fig. 1) [1,2,36]. In vector ordering each multichannel sample or vector $\mathbf{x}_i$, for $i = 1, 2, \ldots, N$, is reduced to a scalar representative ξ_i obtained through the aggregated distances or the aggregated similarities as follows [1,2]:

$$\xi_i(\mathbf{x}_i) = \sum_{j=1}^{N} f(\mathbf{x}_i, \mathbf{x}_j), \tag{1}$$

where $f(\cdot)$ denotes the used distance or dissimilarity function.

To order the color vectors $\mathbf{x}_i$ located inside the supporting window W, the scalar quantities $\xi_1, \xi_2, \ldots, \xi_N$ are ranked in the order of their value and the associated vectors are correspondingly ordered as follows:

$$\xi_{(1)} \leqslant \xi_{(2)} \leqslant \cdots \leqslant \xi_{(N)}, \tag{2}$$

$$\mathbf{x}_{(1)}(\xi_{(1)}) \leqslant \mathbf{x}_{(2)}(\xi_{(2)}) \leqslant \cdots \leqslant \mathbf{x}_{(N)}(\xi_{(N)}), \tag{3}$$

where $\xi_{(i)} \in \{\xi_1, \xi_2, \ldots, \xi_N\}$ and $\mathbf{x}_{(i)} \in \{\mathbf{x}_1, \mathbf{x}_2, \ldots, \mathbf{x}_N\}$, for $i = 1, 2, \ldots, N$. Thus, all the components are given equal importance and the ordered vectors $\mathbf{x}_{(i)}$ have a one-to-one correspondence with the original samples inside W.

[3] Color images are typical examples of multichannel signals. A color image represented by the three primaries in the red–green–blue (RGB) color space is a two-dimensional, three-channel signal with parameters l and m equal to 2 and 3, respectively.

The output of the ranking procedure depends on the type of data from which the computation is to be made, and the function $f(\mathbf{x}_i, \mathbf{x}_j)$ selected to evaluate the dissimilarity or distance between two vectors $\mathbf{x}_i$ and $\mathbf{x}_j$. According to the used feature, it is possible to differentiate the techniques operating on the magnitude domain [19,20,37,38], angular (directional) domain [21,22,39,40], or their combination [41,42,43].

2.1. Vector median filter

Let us consider that each input multichannel sample $\mathbf{x}_i$, for $i = 1, 2, \ldots, N$, is associated with the aggregated distance

$$L_i = \sum_{j=1}^{N} \|\mathbf{x}_i - \mathbf{x}_j\|_\gamma = \sum_{j=1}^{N} \left(\sum_{k=1}^{m} |x_{ik} - x_{jk}|^\gamma \right)^{\frac{1}{\gamma}}, \tag{4}$$

where $\|\mathbf{x}_i - \mathbf{x}_j\|_\gamma$ quantifies the distance among two m-channel samples $\mathbf{x}_i = (x_{i1}, x_{i2}, \ldots, x_{im})$ and $\mathbf{x}_j = (x_{j1}, x_{j2}, \ldots, x_{jm})$ using the generalized Minkowski metric [1,44] with the used norm γ. Note that the Minkowski metric includes [2] the city-block distance ($\gamma = 1$), Euclidean distance ($\gamma = 2$), and chess-board distance ($\gamma = \infty$) as the special cases. Sample $\mathbf{x}_{(1)} \in W$ associated with the minimum vector distance $L_{(1)} \in \{L_1, L_2, \ldots, L_N\}$ constitutes the output of the vector median filter (VMF) [19,45] minimizing the distance to other samples inside the sliding filtering window W.

2.2. Basic vector directional filter

In the directional processing of color images [21,22,25,39,40,46], each input color vector $\mathbf{x}_i$, for $i = 1, 2, \ldots, N$, is associated with the aggregated angular distance

$$\alpha_i = \sum_{j=1}^{N} A(\mathbf{x}_i, \mathbf{x}_j) = \sum_{j=1}^{N} \arccos \left(\frac{\sum_{k=1}^{m} x_{ik} x_{jk}}{\sqrt{\sum_{k=1}^{m} x_{ik}^2} \sqrt{\sum_{k=1}^{m} x_{jk}^2}} \right), \tag{5}$$

where $A(\mathbf{x}_i, \mathbf{x}_j)$ represents the angle between two m-dimensional vectors $\mathbf{x}_i$ and $\mathbf{x}_j$.

The sample $\mathbf{x}_{(1)} \in W$ associated with the minimum angular distance $\alpha_{(1)} \in \{\alpha_1, \alpha_2, \ldots, \alpha_N\}$, i.e., the sample minimizing the sum of angles with other vectors, represents the output of the basic vector directional filter (BVDF) [21]. The set of the r first terms of (3) associated with the smallest aggregated angular distances (5) constitutes an output of the generalized vector directional filter (GVDF) [21], which is often accompanied with an additional filter processing the samples $\mathbf{x}_{(1)}, \mathbf{x}_{(2)}, \ldots, \mathbf{x}_{(r)}$ according to their magnitude. Thus, the GVDF splits the color image processing into the directional processing and the magnitude processing [1]. The drawback of such an approach is that it increases the computational complexity of the VDFs.

2.3. Directional distance filter

Combining both ordering criteria (4) and (5) is followed by directional distance filter (DDF) [43] and hybrid vector filters (HVFs) [42], however, both approaches are rather computationally demanding. HVFs require the evaluation of both the VMF and BVDF outputs and thus, the two independent ordering schemes are applied to the input samples to produce a unique final output.

In the case of DDF associated with the power parameter p ranged from 0 to 1, hybrid ordering criterion expressed through a product of aggregated magnitude (4) and angular (5) distances is given by $\Omega_i = L_i^{1-p} \cdot \alpha_i^p$, for $i = 1, 2, \ldots, N$. The above criterion can be expressed equivalently as follows:

$$\Omega_i = \left(\sum_{j=1}^{N} \|\mathbf{x}_i - \mathbf{x}_j\|_\gamma \right)^{1-p} \cdot \left(\sum_{j=1}^{N} A(\mathbf{x}_i, \mathbf{x}_j) \right)^{p} \quad \text{for } i = 1, 2, \ldots, N. \tag{6}$$

The DDF output is the sample $\mathbf{x}_{(1)} \in W$ minimizing (6), i.e., the sample associated with the smallest value $\Omega_{(1)} \in \{\Omega_1, \Omega_2, \ldots, \Omega_N\}$. If $p = 0$, then the DDF operates as the VMF, whereas for $p = 1$ the DDF is equivalent to the BVDF.

3. Proposed framework

Standard vector filtering schemes such as VMF, BVDF, and DDF operating on a fixed supporting window introduce excessive smoothing, blur image details, and eliminate fine image structures. This undesired property is caused by the excessive smoothing capability of a low-pass filtering affecting the textured regions. To avoid excessive smoothing and preserve image details, the noise reduction filters should be designed so that noise-free samples remain unchanged during the filtering operation. There are at least three possible ways to accomplish this task using a filter that operates on a fixed supporting window:

(1) To increase the degree of freedom in the design by introducing parameters into the filter structure. Usually, the increased number of filter coefficients under the training procedure improves the possibility to enhance the desired signal. The two extremes represented by simple weighted filtering framework [25–27] (mostly derived from scalar weighted medians [23,5] and stack filters [5,7,23,24]) and the permutation filtering classes [5,47] follow this directions. The drawback of such filters lies in the relatively complex optimization approaches, their computational complexity (especially in permutation theory-based approaches) and the training of a high number of filter parameters, which can lead to decreased filter robustness.
(2) To incorporate structural information to the filter design. This way follows weighted median optimization-based structural approaches. Some recent designs [28,29] propose to use adaptively changed direction of the filter operating sub-window as a tool to control and decrease the excessive smoothing. Other previously published approaches [30,48] deal with nontraditional window shapes along the image samples of similar intensities which form the digital paths [30] on the image domain.
(3) To introduce a switching rule [20,33–35,39,37] allowing the filter to switch between the robust nonlinear filter (such as VMF) and the identity operation. Thus, in the case of noise-free samples, the filter retains the samples unchanged (identity operation). Noisy samples are replaced by the output of the nonlinear smoothing filter. Such an adaptive filter belongs to the switching filtering classes.

In this paper, we focus on the multichannel switching filtering. This filtering approach is useful for detection and removal of the noise in a wide range of applications, where the preservation of the desired structures and color information is of a paramount importance. Such applications include television [17], video [12], HDTV and also new emerging fields such as DNA microarrays processing [8,9], reconstruction of digitized fine arts [10], automatic systems of visual inspection in transportation [15] or quality control, etc. We will show the efficiency of the proposed framework in Section 4 and will compare its efficiency with the performance of standard filtering schemes as well as some relevant adaptive extensions.

Although a number of switching approaches [31–35,37,39,46] have been proposed to date, a majority of them focuses on outliers detection in gray-scale images. Another problem related to switching filters can be often observed with respect to their inefficient robustness [31], high computational complexity [35,39], complex optimization [33,46], high number of switching levels [34], and low flexibility to accommodate the algorithm for a variety of window shapes [33,35].

In this paper, we provide a new multichannel filtering framework based on order-statistic theory and statistical switching using standard deviation or approximation of the variance both computed using the input samples spawned by a filtering window. The paper extends the preliminary results presented in our previous works [49–52]. Incorporating the statistical operators evaluated over the multichannel samples is a unique and distinguishing element in the presented work. Furthermore, the proposed framework is flexible, it can be designed to use advantages of basic filtering operators such as the sample mean and the lowest ranked vector, provides more degree of freedom than the standard multichannel filtering schemes, and generalizes the VMF-based switching filter in [52]. Moreover, the proposed method can be easily adapted for a large window size without any additional effort.

Fig. 2 shows the concept of the approximation of multivariate variance. The radius of the circles denotes the approximation of the variance or rather product of variance and a control parameter. If the central pixel is inside the circle then it is noise-free, otherwise the central sample is an outlier. Note that two ways are possible: radius of the circles with centers in the lowest ranked vector (robust estimate in impulsive environments) and in the sample mean. Similar procedure was used by Lee [32], who applied the concept for the gray-scale images computing a weighted average over the filter window. This procedure computes a weighted mean over the filter window, but only those pixels whose values lie within the variance of the central pixel value (or rather the variance multiplied by the tuning parameter λ) are taken into the average. Note that λ is a control element in such a design and Lee suggested that λ should be around two. This filter attempts to estimate a new pixel value with only those neighbors, whose values do not deviate too much from the value of the central sample.

Such a simple control can be also considered as the base for the decision stated multichannel filtering. In order to provide the adaptive trade-off between the identity filter (no smoothing) and the robust multichannel filtering techniques, e.g., VMF or its derivatives, we present first a filtering scheme called vector sigma filter which makes use of the distances between the vector samples contained in the filtering window. Note that in terms of VMF, BVDF, and DDF definitions, we describe sigma VMF (SVMF) filters [52] and extend this concept in order to introduce sigma BVDF (SBVDF) and sigma DDF (SDDF) filters. These filtering schemes are controlled by a tuning parameter λ and take advantages of the standard sigma-filter concept (Fig. 2) and the approximation of the variance in the multivariate case [52]. Although the adaptation of the tuning parameter can be easily performed and the methods are sufficiently robust, in order to follow the fully adaptive filtering schemes (optimization and parameter free) we also provide the adaptive vector sigma filters [49–51], called adaptive sigma VMF (ASVMF), adaptive sigma BVDF (ASBVDF), and adaptive sigma DDF (ASDDF) based on the standard deviation of the input set.

The measure of the multivariate samples is very often defined by the variance–covariance matrix $\mathbf{\Sigma}$ of the samples $\mathbf{x} = \{\mathbf{x}_1, \mathbf{x}_2, \ldots, \mathbf{x}_N\}$ defined as

$$\begin{aligned}\mathbf{\Sigma} &= E[(\mathbf{x} - \bar{\mathbf{x}}) \cdot (\mathbf{x} - \bar{\mathbf{x}})] \\ &= \begin{pmatrix} \mathrm{var}(R) & \mathrm{cov}(R,G) & \mathrm{cov}(R,B) \\ \mathrm{cov}(G,R) & \mathrm{var}(G) & \mathrm{cov}(G,B) \\ \mathrm{cov}(B,R) & \mathrm{cov}(B,G) & \mathrm{var}(B) \end{pmatrix},\end{aligned} \tag{7}$$

where R, G, and B denote the red, green, and blue color pixel channels, E is the expected value operator, and $\bar{\mathbf{x}}$ denotes the arithmetic mean of the vector samples. In this way

$$\mathbf{\Sigma} = \begin{pmatrix} \sigma_{RR} & \sigma_{RG} & \sigma_{RB} \\ \sigma_{GR} & \sigma_{GG} & \sigma_{GB} \\ \sigma_{BR} & \sigma_{BG} & \sigma_{BB} \end{pmatrix}, \tag{8}$$

where $\sigma_{k,k}$ is the standard deviation of the values of the channel k. The dispersion matrix $\mathbf{\Sigma}$ is square, symmetric and usually of full rank.

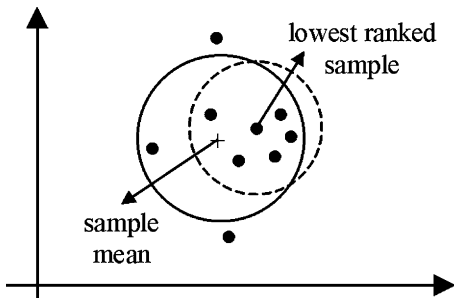

Fig. 2. The concept of the sigma filtering in the two-dimensional case, where we indicate that the radius is the variance or rather variance multiplied by the tuning parameter λ.

In many applications, it is very useful to use a scalar value capturing the multivariate data dispersion. One of the ways of introducing such a scalar measure is the so-called generalized variance $|\mathbf{\Sigma}|$ defined as the determinant of the $\mathbf{\Sigma}$ matrix, which can be calculated as the product of the eigenvalues of $\mathbf{\Sigma}$ [53]. The idea is to measure the volume occupied by the multivariate variables in $|\mathbf{\Sigma}|$. The multivariate dispersion can also be given as a sum of the eigenvalues of the variance–covariance matrix, (total variance) [54].

The former plays an important role in maximum likelihood estimation and model selection and the latter is used as a measure of variation in principal components analysis [55–57].

These dispersion measures well describe the samples' variability, but their drawback is that these methods are computationally very expensive and thus inappropriate for image processing. That is why we make use of simple but effective dispersion measures based on the sample mean and vector median: multivariate variance measured from the sample mean and variance measured from the sample vector median.

3.1. Vector sigma filters

In this subsection, determining the range for the detection of noisy samples will depend on approximation of the variance of the input multichannel sample. Thus, we avoid the computational difficulties connected with calculation of variance–covariance matrices and provide a simple way to follow the concept shown in Fig. 2.

3.1.1. Design based on the lowest ranked vector

Let ψ_γ be the approximation of the multivariate variance of the vectors contained in a supporting window W of sufficiently large window size N (number of pixels in the filter window W), given by

$$\psi_\gamma = \frac{L_{(1)}}{N-1}, \tag{9}$$

where $L_{(1)} = \sum_{j=1}^{N} \|\mathbf{x}_{(1)} - \mathbf{x}_j\|_\gamma$ is the aggregated distance calculated by (4) and associated with the vector median $\mathbf{x}_{(1)}$. This approximation represents the mean distance between the vector median and all other color pixels contained in W. The division of smallest aggregated distance $L_{(1)}$ by $N-1$ (number of distances from $\mathbf{x}_{(1)}$ to all samples from W) ensures that the dispersion measure is nondependent on the filtering window size.

Following the switching concept in [52], the SVMF uses the threshold Tol defined as follows:

$$Tol = L_{(1)} + \lambda\psi_\gamma = \frac{N-1+\lambda}{N-1} L_{(1)}, \tag{10}$$

where $L_{(1)}$ is the smallest aggregated Minkowski metric, ψ_γ is the approximated variance, and λ is the tuning parameter used to adjust the smoothing properties of the SVMF.

If the threshold Tol is compared with the distance measure $L_{(N+1)/2}$ of the center pixel $\mathbf{x}_{(N+1)/2}$, it is possible to derive a simple switching rule for the replacement of noisy pixels [52]:

$$\mathbf{y}_{\mathrm{SVMF}} = \begin{cases} \mathbf{x}_{(1)} & \text{for } L_{(N+1)/2} \geqslant Tol, \\ \mathbf{x}_{(N+1)/2} & \text{otherwise}, \end{cases} \tag{11}$$

where $\mathbf{y}_{\mathrm{SVMF}}$ is the SVMF output, $L_{(N+1)/2}$ denotes the distance measure of the center pixel $\mathbf{x}_{(N+1)/2}$ as explained in (4), and $\mathbf{x}_{(1)}$ is the VMF output.

If the distance measure $L_{(N+1)/2}$ of the central sample $\mathbf{x}_{(N+1)/2}$ is larger or equal to the threshold Tol, then $\mathbf{x}_{(N+1)/2}$ is most probably noisy and is being replaced with the lowest ranked vector $\mathbf{x}_{(1)}$ (see Fig. 2). If the distance measure $L_{(N+1)/2}$ of the central sample $\mathbf{x}_{(N+1)/2}$ is smaller than the threshold Tol, then $\mathbf{x}_{(N+1)/2}$ is similar to other input samples, which indicates that $\mathbf{x}_{(N+1)/2}$ is most probably noise-free and is kept unchanged (no filtering operation is performed).

From (11) it is not difficult to see that the filtering result depends on the tuning parameter λ. If $\lambda = 0$, then the filter output is always the VMF. On the other hand, for big values of λ the framework will always output the central pixel $\mathbf{x}_{(N+1)/2}$ according to the following expression:

$$\mathbf{y} = \begin{cases} \mathbf{x}_{(1)} & \text{if } \lambda = 0, \\ \mathbf{x}_{(N+1)/2} & \text{if } \lambda \to \infty. \end{cases} \tag{12}$$

Since $L_{(N+1)/2} = L_{(1)} + \Delta$, it can be easily shown [52] that $\Delta/L_{(1)} \geqslant \lambda/(N-1)$. From this expression it is clear that the proposed method will perform the identity operation for any value of λ, if and only if the lowest ranked vector $\mathbf{x}_{(1)}$ is identical with the central sample $\mathbf{x}_{(N+1)/2}$ and thus $\Delta = 0$. This property is interesting in the context of deterministic properties usually expressed through the analysis of root signals. If $\mathbf{x}_{(1)} \neq \mathbf{x}_{(N+1)/2}$ then the SVMF output is a root if and only if the ratio $\Delta/L_{(1)}$ is larger than or equal to the tuning element $\lambda/(N-1)$. Note that the second extreme for the identity operation can be expressed by

$$(N-2)(N-1) \geqslant \lambda \tag{13}$$

which means that an additional increasing of λ, e.g., up to 56 in the case of a 3×3 filtering window, makes the filter idempotent. With respect to this analysis, we provide Fig. 3 which shows the dependency of boundary values λ on window size N to achieve the identity operation. The interested reader should refer to [52] for additional analysis of the SVMF method.

In the same way as in the SVMF approach defined by (9)–(11), it is possible to derive the proposed SBVDF and SDDF filters. In the case of the SBVDF technique, Eqs. (9)–(11) should be modified as follows:

$$\psi_{\mathrm{A}} = \frac{\alpha_{(1)}}{N-1}, \tag{14}$$

$$Tol = \alpha_{(1)} + \lambda\psi_{\mathrm{A}}, \tag{15}$$

$$\mathbf{y}_{\mathrm{SBVDF}} = \begin{cases} \mathbf{x}_{(1)} & \text{for } \alpha_{(N+1)/2} \geqslant Tol, \\ \mathbf{x}_{(N+1)/2} & \text{otherwise}, \end{cases} \tag{16}$$

where $\alpha_{(1)}$ is the smallest aggregated angular distance (5), ψ_{A} is the approximated variance computed using the angular distance of multichannel samples inside the filtering window, and $\mathbf{x}_{(1)}$ is the result of BVDF operation. The vector $\mathbf{y}_{\mathrm{SBVDF}}$ is the SBVDF output that depends on the comparison of the aggregated angular distance $\alpha_{(N+1)/2}$ related to the central input sample $\mathbf{x}_{(N+1)/2}$ with the threshold value Tol.

If the generalized SDDF filtering structure is considered, the approximated variance $\psi_{\gamma\mathrm{A}}$ is given by

$$\psi_{\gamma\mathrm{A}} = \frac{\Omega_{(1)}}{N-1} \tag{17}$$

where $\Omega_{(1)}$ is the smallest hybrid measure in (6). Then, the threshold value is expressed as

$$Tol = \Omega_{(1)} + \lambda\psi_{\gamma\mathrm{A}} \tag{18}$$

and the SDDF output $\mathbf{y}_{\mathrm{SDDF}}$ is defined by

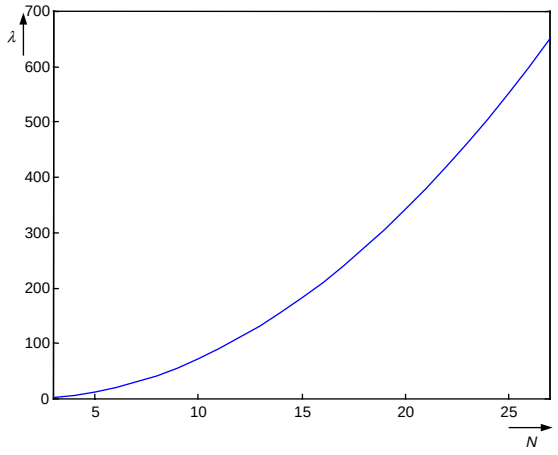

Fig. 3. Dependence of boundary value of λ on window size N.

$$\mathbf{y}_{\mathrm{SDDF}} = \begin{cases} \mathbf{x}_{(1)} & \text{for } \Omega_{(N+1)/2} \geqslant Tol, \\ \mathbf{x}_{(N+1)/2} & \text{otherwise,} \end{cases} \tag{19}$$

where $\mathbf{x}_{(1)}$ characterizes the DDF operation related to power parameter p and $\Omega_{(N+1)/2}$ is the aggregated hybrid measure (6) associated with the central input sample $\mathbf{x}_{(N+1)/2}$.

It is clear that the SDDF holds the same generalization for SVMF and SBVDF filters as the DDF for VMF and BVDF techniques. It means that the SDDF can perform the SVMF filtering (for $p = 0$) and the SBVDF filtering (for $p = 1$), whereas for $p = 0.5$ the filter is equivalent to the standard SDDF filter. Varying the power parameter p, it is possible to control the influence of magnitude and angular domain in the SDDF switching stage and also to tune the smoothing properties of the DDF technique in the second filtering stage. In addition, the smoothing capability of the SDDF technique is also controlled by the tuning parameter λ (see Eq. (12)), which increases the degree of freedom of the SDDF technique in comparison with the standard DDF approach. From (12) and (19) it can be observed that for $\lambda = 0$ the SDDF is equivalent to the standard DDF approach, whereas for $\lambda \to \infty$ the SDDF will perform the identity operation (no filtering) and will keep all input data unchanged. If the tuning parameter $\lambda = 0$, the SDDF smoothing capability depends only on the power parameter p, and the VMF and BVDF filtering can be obtained for $p = 0$ and $p = 1$, respectively, as special cases. For that reason, the introduction of the SDDF structure extends the design possibilities of multichannel filters and represents the generalization of the above-mentioned filtering techniques as well as our initial SVMF design in [52]. In addition to this analysis, the SDDF and also SBVDF behavior corresponds to the analysis shown in Fig. 3 as well as to additional analysis provided in [52].

The proposed sigma vector filters (SVMF, SBVDF, and SDDF) are computationally efficient, since they perform practically the same number of operations as their nonadaptive special cases such as VMF, BVDF, and DDF. Comparing the construction of the generalized algorithms shown in Figs. 1 and 4 reflects that both schemes need to compute the aggregated distances and search for the minimum of them. The switching rule

```
Inputs:  NumberOfRows × NumberOfColumns noisy image
         Window size N
         Moving window spawning the input set {x_1, x_2, ..., x_N}
         Tuning parameter λ
Output:  NumberOfRows × NumberOfColumns image

For a = 1 to NumberOfRows
  For b = 1 to NumberOfColumns
    Determine the input set W(a,b) = {x_1, x_2, ..., x_N}
    For i = 1 to N
      For j = 1 to N
        Compute the distance f(x_i, x_j)
      end
      Compute the sum ξ_i = f(x_i, x_1) + f(x_i, x_2) + ... + f(x_i, x_N)
    end
    Sort ξ_1, ξ_2, ..., ξ_N to the ordered set ξ_(1) ≤ ξ_(2) ≤ ... ≤ ξ_(N)
    Compute Tol = ξ_(1) + λξ_(1) /(N − 1)
    If ξ_((N+1)/2) ≥ Tol
      Apply the same ordering to x_1(ξ_1), x_2(ξ_2), ..., x_N(ξ_N)
      Store ordered sequence as x_(1) ≤ x_(2) ≤ ... ≤ x_(N)
      Let the filter output y(a,b) = x_(1)
    Else
      Let the filter output y(a,b) = x_((N+1)/2)
  End
End
```

Fig. 4. Algorithm of the vector sigma filter.

requires division, multiplication, and addition, however, in the case of noise-free sample (majority of cases), no additional processing is necessary. If an outlier is detected, the rest of operations is the same as in the case of standard filtering schemes VMF, BVDF, and DDF. Finally, it should be mentioned that the SVMF is the most computationally attractive case of the SDDF filtering.

3.1.2. Design based on the sample mean

In order to follow both concepts shown in Fig. 2, we can achieve a new approach which is more computationally attractive than the discussed previously. Replacing the lowest ranked vector with the sample mean in the switching stage of the proposed method, we avoid the calculation of aggregated distances of input samples to other samples of the input set and searching for the minimum distance and the lowest ranked vector. However, the sample mean is not as robust operator in impulsive environments as the lowest ranked sample, and thus, we expect that this modification will not be so efficient as the previous ''ranked'' method, in the case of heavily corrupted environments.

Let us consider the generalized DDF filtering scheme and the variance approximated by

$$\psi_{\gamma \mathrm{A}} = \frac{\Omega_{\bar{\mathbf{x}}}}{N}, \tag{20}$$

where

$$\Omega_{\bar{\mathbf{x}}} = \left(\sum_{j=1}^{N} \|\bar{\mathbf{x}} - \mathbf{x}_j\|_{\gamma} \right)^{1-p} \left(\sum_{j=1}^{N} A(\bar{\mathbf{x}}, \mathbf{x}_j) \right)^{p} \tag{21}$$

is the aggregated measure between multichannel input samples $\mathbf{x}_1, \mathbf{x}_2, \ldots, \mathbf{x}_N$ and the sample mean $\bar{\mathbf{x}}$ defined by

$$\bar{\mathbf{x}} = \frac{1}{N} \sum_{i=1}^{N} \mathbf{x}_i. \tag{22}$$

Following the definition in (19), the output of the proposed mean-based SDDF filtering scheme is given by

$$\mathbf{y}_{\mathrm{SDDF}} = \begin{cases} \mathbf{x}_{(1)} & \text{for } \Omega_{(N+1)/2} \geqslant Tol_{\bar{x}}, \\ \mathbf{x}_{(N+1)/2} & \text{otherwise}, \end{cases} \tag{23}$$

where $Tol_{\bar{x}}$ is the threshold value defined like in the ranking-based SDDF approach, which results in

$$Tol_{\bar{x}} = \frac{N+\lambda}{N} \Omega_{\bar{\mathbf{x}}}. \tag{24}$$

It is clear that mean-based SDDF scheme in (23) holds the same generalization as their ranking-based equivalent in (19). Since $\bar{\mathbf{x}}$ is generally closer to multichannel samples than the lowest ranked vector we expect that the sub-optimal value of λ will be larger than that of the ranking-based SDDF approach.

3.2. Adaptive vector sigma filters

The smoothing capability of the SDDF approaches especially depends on the tuning parameter λ, whereas the power parameter p can be considered as the generalization parameter like in the DDF design. Although the adaptation of the tuning parameter can be performed easily and the methods are sufficiently robust, in order to follow the fully adaptive filtering paradigm, we also provide the so-called adaptive vector sigma filters (Fig. 5) [49–51], such as adaptive sigma VMF (ASVMF), adaptive sigma BVDF (ASBVDF), and adaptive sigma DDF (ASDDF). Besides the fully adaptive structure, another advantage of the proposed scheme is related to the exclusion of the time-consuming ordering operation used in ranking-based vector sigma filters, when the desired sample is detected by a switching filter stage.

3.2.1. Design based on the sample mean

Let us consider a population of the scalar samples $x_1, x_2, \ldots, x_N$ and their variance σ^2 given by

```
Inputs:  NumberOfRows × NumberOfColumns noisy image
         Window size N
         Moving window spawning the input set {x_1, x_2, ..., x_N}
Output:  NumberOfRows × NumberOfColumns image

For a = 1 to NumberOfRows
  For b = 1 to NumberOfColumns
    Determine the input set W(a,b) = {x_1, x_2, ..., x_N}
    Compute the mean x̄ of the input set {x_1, x_2, ..., x_N}
    For i = 1 to N
      Compute the distance f(x_i, x̄)
    end
    Compute the variance σ^2 = (f^2(x_1, x̄) + f^2(x_2, x̄) + ... + f^2(x_N, x̄))/N
    If f(x_(N+1)/2, x̄) ≥ σ
      For i = 1 to N
        For j = 1 to N
          Compute the general distance f(x_i, x_j)
        end
        Compute the sum ξ_i = f(x_i, x_1) + f(x_i, x_2) + ... + f(x_i, x_N)
      end
      Sort ξ_1, ξ_2, ..., ξ_N to the ordered set ξ_(1) ≤ ξ_(2) ≤ ... ≤ ξ_(N)
      Apply the same ordering to x_1(ξ_1), x_2(ξ_2), ..., x_N(ξ_N)
      Store ordered sequence as x_(1) ≤ x_(2) ≤ ... ≤ x_(N)
      Let the filter output y(a,b) = x_(1)
    Else
      Let the filter output y(a,b) = x_(N+1)/2
  End
End
```

Fig. 5. Algorithm of the adaptive vector sigma filter.

$$\sigma^2 = \frac{1}{N}\sum_{i=1}^{N}(x_i - \bar{x})^2, \tag{25}$$

where $\bar{x}$ is the mean of the observed data and N is the number of the samples. The square root of the variance, σ, is the standard deviation.

If the variance σ^2 is generalized for a vector case applied to the input set of multichannel samples $\mathbf{x}_1, \mathbf{x}_2, \ldots, \mathbf{x}_N$, then [49]:

$$\sigma_\gamma^2 = \frac{1}{N}\sum_{i=1}^{N}(\|\mathbf{x}_i - \bar{\mathbf{x}}\|_\gamma)^2, \tag{26}$$

where N is the window size, γ denotes the chosen norm (e.g., Euclidean for $\gamma = 2$), and $\bar{\mathbf{x}}$ is the mean of multichannel data $\mathbf{x}_1, \mathbf{x}_2, \ldots, \mathbf{x}_N$ given by (22).

In this way, the angular definition of the multichannel variance [50] is given by

$$\sigma_{\mathrm{A}}^2 = \frac{1}{N}\sum_{i=1}^{N}A^2(\mathbf{x}_i, \bar{\mathbf{x}}), \tag{27}$$

where $A(\cdot)$ denotes the angle between multichannel samples.

In terms of the DDF filter structure, the combination of σ_γ^2 and σ_{A}^2 is expressed [51] as follows $\sigma_{\gamma\mathrm{A}}^2 = (\sigma_\gamma^2)^{1-p}(\sigma_{\mathrm{A}}^2)^p$ which can be rewritten as:

$$\sigma_{\gamma \mathrm{A}}^2 = \left(\frac{1}{N} \sum_{i=1}^{N} (\|\mathbf{x}_i - \bar{\mathbf{x}}\|_\gamma)^2 \right)^{1-p} \left(\frac{1}{N} \sum_{i=1}^{N} A^2(\mathbf{x}_i, \bar{\mathbf{x}}) \right)^p, \tag{28}$$

where p is the same power parameter as in the DDF structure.

Calculating the difference ς_γ between the central sample $\mathbf{x}_{(N+1)/2}$ and the sample mean $\bar{\mathbf{x}}$ using

$$\varsigma_\gamma = \|\mathbf{x}_{(N+1)/2} - \bar{\mathbf{x}}\|_\gamma \tag{29}$$

and also the angle ς_{A} between $\mathbf{x}_{(N+1)/2}$ and $\bar{\mathbf{x}}$ using

$$\varsigma_{\mathrm{A}} = A(\mathbf{x}_{(N+1)/2}, \bar{\mathbf{x}}) \tag{30}$$

the difference between $\mathbf{x}_{(N+1)/2}$ and $\bar{\mathbf{x}}$ can be expressed through the combined measure [51] as $\varsigma_{\gamma A} = (\varsigma_\gamma)^{1-p}(\varsigma_{\mathrm{A}})^p$ or as follows:

$$\varsigma_{\gamma \mathrm{A}} = \left(\left\| \mathbf{x}_{(N+1)/2} - \bar{\mathbf{x}} \right\|_\gamma \right)^{1-p} \left(A(\mathbf{x}_{(N+1)/2}, \bar{\mathbf{x}}) \right)^p. \tag{31}$$

Thus, the corruption of $\mathbf{x}_{(N+1)/2}$ is determined through the comparison of $\sigma_{\gamma \mathrm{A}}$ and $\varsigma_{\gamma \mathrm{A}}$ which forms the following outlier detection rule [51]: $\varsigma_{\gamma \mathrm{A}} \geqslant \sigma_{\gamma \mathrm{A}}$. If the combined measure $\varsigma_{\gamma \mathrm{A}}$ is greater than or equal to a square root of the combined variance $\sigma_{\gamma \mathrm{A}}^2$, then the central sample $\mathbf{x}_{(N+1)/2}$ is probably noisy because the corresponding combined measure (6) reflects the significant difference between $\mathbf{x}_{(N+1)/2}$ and its neighborhoods. The high similarity between $\mathbf{x}_{(N+1)/2}$ and the input set $\mathbf{x}_1, \mathbf{x}_2, \ldots, \mathbf{x}_N$ is reflected by $\varsigma_{\gamma \mathrm{A}} < \sigma_{\gamma \mathrm{A}}$.

When the above-mentioned rule is introduced to the DDF filter structure, the output of the proposed adaptive sigma DDF (ASDDF) method is given by

$$\mathbf{y}_{\mathrm{ASDDF}} = \begin{cases} \mathbf{x}_{(1)} & \text{for } \varsigma_{\gamma \mathrm{A}} \geqslant \sigma_{\gamma \mathrm{A}}, \\ \mathbf{x}_{(N+1)/2} & \text{otherwise}, \end{cases} \tag{32}$$

where $\mathbf{x}_{(1)}$ characterizes the DDF output minimizing the hybrid measure (6) and $\mathbf{x}_{(N+1)/2}$ is the input central sample.

It is clear that the standard DDF operation is performed when the condition $\varsigma_{\gamma A} \geqslant \sigma_{\gamma \mathrm{A}}$ is satisfied, i.e., the effect of the DDF filtering is restricted only to noisy samples. If $\varsigma_{\gamma \mathrm{A}} < \sigma_{\gamma \mathrm{A}}$, then $\mathbf{x}_{(N+1)/2}$ is similar to other input samples and remains unchanged. For $p = 0$ the ASDDF method is equivalent to the adaptive sigma VMF (ASVMF) filter [49], whereas for $p = 1$ it performs the adaptive sigma BVDF (ASBVDF) filtering [50], i.e., the angular multichannel generalization of the proposed adaptive filtering.

Concerning the computational complexity, the adaptive vector sigma filters (Fig. 5) are computationally very efficient and they significantly decrease the number of operations typical for standard filtering schemes (Fig. 1) and ranking-based vector sigma filters (Fig. 4). In each cycle, adaptive vector sigma filters need to determine the sample mean like in mean-based vector sigma filters (23), square root of the variance of the input set, and the distance between the central sample and the sample mean. However, the crucial advantage of the ASVMF, ASBVDF, and ASDDF is displayed in the case of noise-free samples, when these filtering schemes allow to omit the operations related to computation of the aggregated distances, searching for the minimum of them and sample ordering. Note that this set of operations is typical for both schemes shown in Figs. 1 and 4. Thus, the detection of noise-free samples using the scheme shown in Fig. 5 is also accompanied with excluding of the most time-consuming operations. Similar to the SVMF, also the ASVMF is the most computationally attractive case of adaptive vector sigma filters.

3.2.2. Design based on the lowest ranked vector

The adaptive vector sigma filters can be also designed in terms of ranking-based filtering scheme. In such a design the output of the ASDDF filter is given by (32), where the multichannel variance $\sigma_{\gamma \mathrm{A}}^2$ and the hybrid difference measure $\varsigma_{\gamma \mathrm{A}}$ are defined as follows:

$$\sigma_{\gamma \mathrm{A}}^2 = \left(\frac{1}{N-1} \sum_{i=1}^{N} \left(\left\| \mathbf{x}_i - \mathbf{x}_{(1)} \right\|_\gamma \right)^2 \right)^{1-p} \left(\frac{1}{N-1} \sum_{i=1}^{N} A^2\left(\mathbf{x}_i, \mathbf{x}_{(1)}\right) \right)^p, \tag{33}$$

$$\varsigma_{\gamma A} = \left(\left\| \mathbf{x}_{(N+1)/2} - \mathbf{x}_{(1)} \right\|_{\gamma} \right)^{1-p} \left(A\left(\mathbf{x}_{(N+1)/2}, \mathbf{x}_{(1)}\right) \right)^{p}. \tag{34}$$

Then, the ranking-based ASDDF scheme with power parameter p covers the ranking-based ASVMF ($p = 0$) and ASBVDF ($p = 1$) schemes as special cases. On the other hand, the introduction of the lowest ranked vector into the switching stage decreases the computational efficiency of such a design.

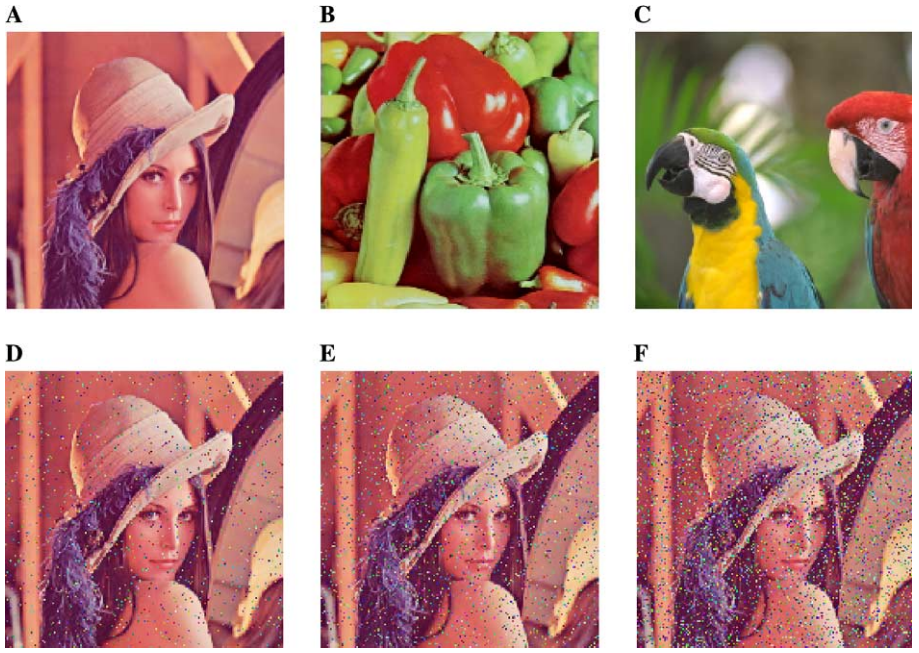

Fig. 6. Experimental results: (A) original image Lena, (B) original image Peppers, (C) original image Parrots, and (D–F) image Lena corrupted by impulsive noise with the probability: (D) $p_v = 0.05$, (E) $p_v = 0.10$, and (F) $p_v = 0.20$.

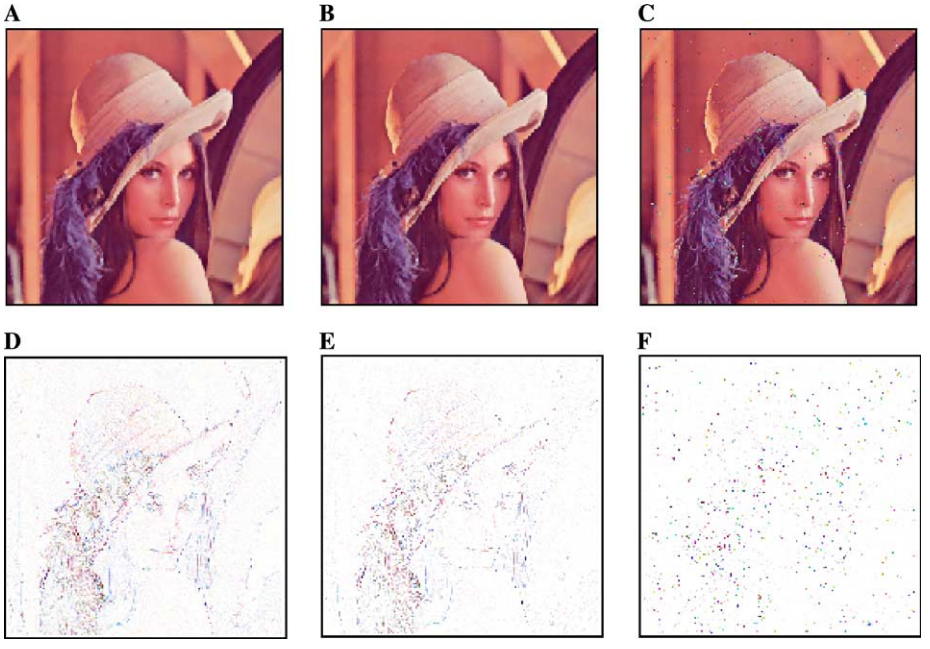

Fig. 7. Filtering results (A–C) and estimation error (D–F) of the SVMF achieved using the test image Lena corrupted by impulsive noise $p_v = 0.10$ (Fig. 6E) in dependence on the tuning parameter λ (A and D) $\lambda = 0.1$, (B and E) $\lambda = 1$, and (C and F) $\lambda = 10$.

Finally, it should be noted that the mean-based ASDDF scheme represents a powerful tool, especially for small p, for the noise detection in removal in color images. In the case of $p < 0.55$, its performance is sufficiently robust [51]. With respect to the general concept with weighted approximated variance used in the SDDF design, ASDDF scheme (32) can be modified as follows:

$$\mathbf{y}_{\mathrm{ASDDF}} = \begin{cases} \mathbf{x}_{(1)} & \text{for } \varsigma_{\gamma \mathrm{A}} \geqslant \lambda \sigma_{\gamma \mathrm{A}}, \\ \mathbf{x}_{(N+1)/2} & \text{otherwise.} \end{cases} \tag{35}$$

Using this structure we extend the design possibilities of the ASDDF and allow to control the switching stage.

4. Experimental results

The primary purpose of all filtering schemes presented in this paper is to remove impulses and outliers from the image. This type of noise corruption is often introduced through bit errors [5], especially during the scanning or transmission over the noisy information channel. Operating on bit-levels of noise-free (original) and noisy (corrupted) components:

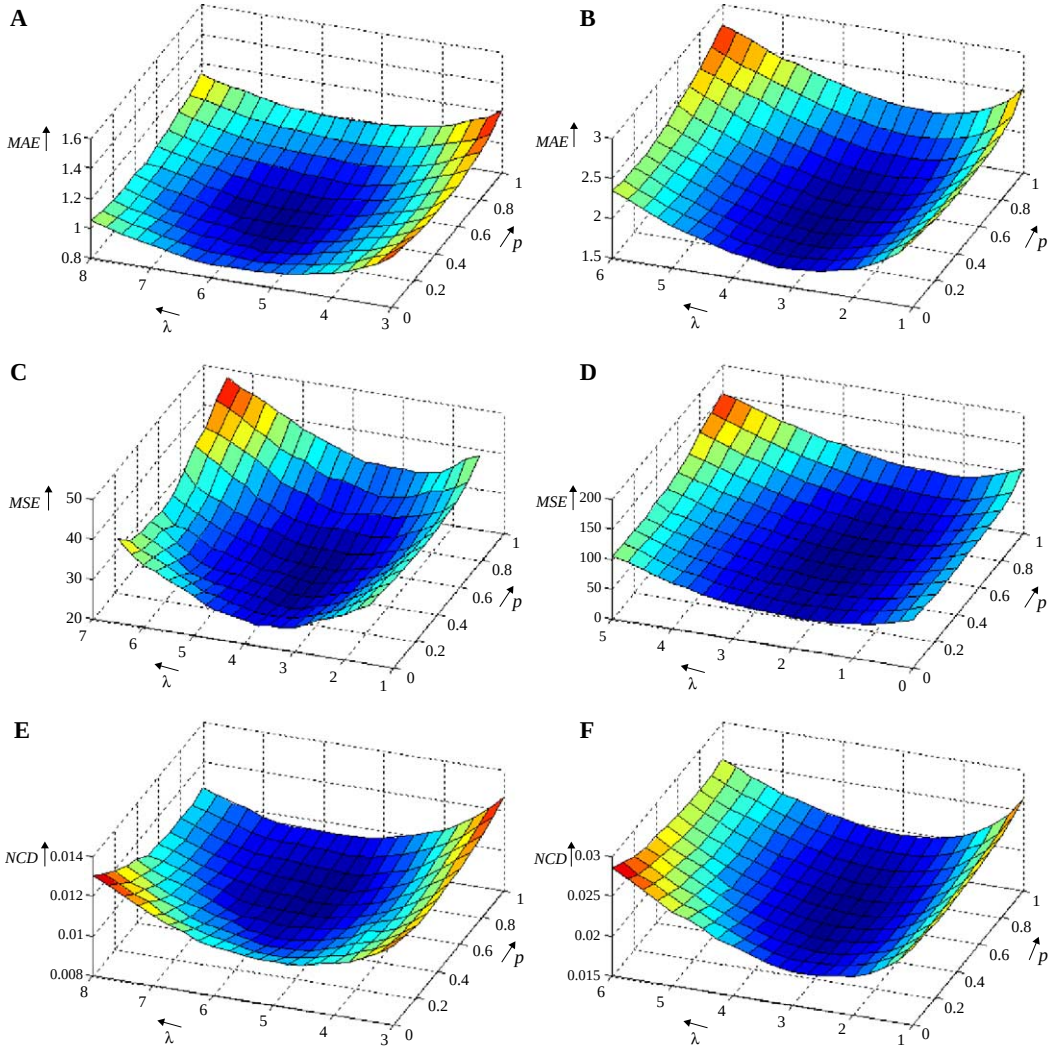

Fig. 8. Performance of the ranking-based SDDF in dependence on power parameter p and tuning parameter λ using the test image Lena corrupted by impulsive noise: (A, C, and E) $p_{\mathrm{v}} = 0.10$, (B, D, and F) $p_{\mathrm{v}} = 0.20$.

$$o_{ik} = o_{ik}^{B-1}2^{B-1} + o_{ik}^{B-2}2^{B-2} + \cdots + o_{ik}^{1}2 + o_{ik}^{0}, \tag{36}$$

$$x_{ik} = x_{ik}^{B-1}2^{B-1} + x_{ik}^{B-2}2^{B-2} + \cdots + x_{ik}^{1}2 + x_{ik}^{0}, \tag{37}$$

respectively, bit-errors like corruption are modeled as follows:

$$x_{ik}^{b} = \begin{cases} o_{ik}^{b} & \text{with probability } 1 - p_v, \\ 1 - o_{ik}^{b} & \text{with probability } p_v, \end{cases} \tag{38}$$

where k denotes the color channel, p_v is the bit-corruption probability, and $b = 0, 1, 2, \ldots, B-1$ denotes the bit-levels of the original and noisy color vectors $\mathbf{o}_i = (o_{ik}, o_{i2}, \ldots, o_{im})$ and $\mathbf{x}_i = (x_{ik}, x_{i2}, \ldots, x_{im})$, respectively. The quantities o_{ik}^{b} and x_{ik}^{b} denote the bth bit ($\{0,1\}$) of o_{ik} and x_{ik} in B-bit per color component representation.

It is not difficult to see that the model in (38) can be simplified to the impulsive noise model defined as follows [41]:

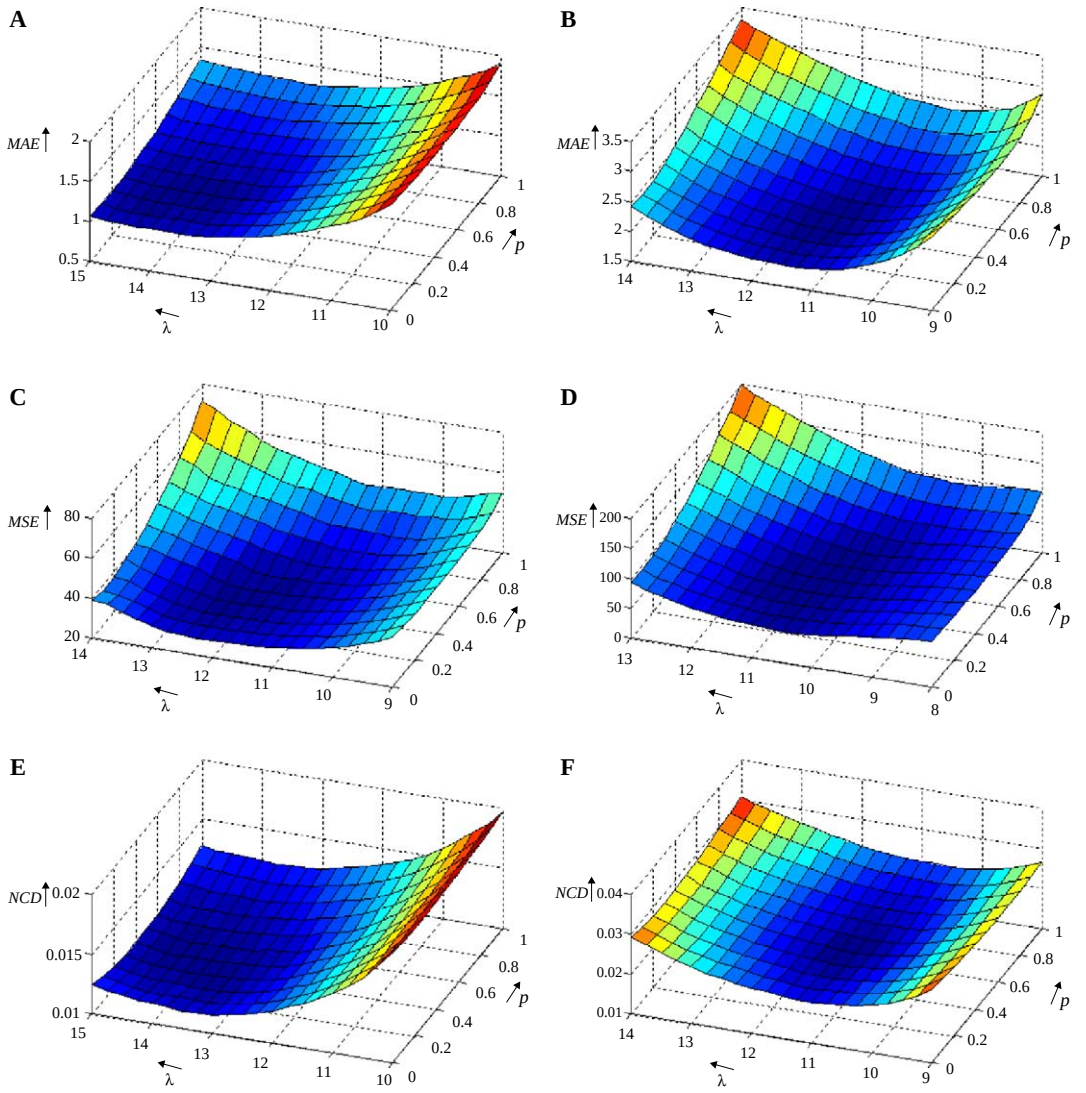

Fig. 9. Performance of the mean-based SDDF in dependence on power parameter p and tuning parameter λ using the test image Lena corrupted by impulsive noise: (A, C, and E) $p_v = 0.10$, (B, D, and F) $p_v = 0.20$.

$$\mathbf{x}_i = \begin{cases} \mathbf{v}_i & \text{with probability } p_{\mathbf{v}}, \\ \mathbf{o}_i & \text{with probability } 1 - p_{\mathbf{v}}, \end{cases} \tag{39}$$

where $\mathbf{o}_i$ is the original sample, $\mathbf{x}_i$ represents the sample from the noisy image, and $p_{\mathbf{v}}$ is a corruption probability. The impulse $\mathbf{v}_i = (v_{i1}, v_{i2}, \ldots, v_{im})$ is usually considered independent from pixel to pixel and has generally much larger (or smaller) amplitude compared to that of neighboring samples at least in one of the spectral components. In this paper, we used the model of impulsive noise in (39) and considered the impulse noise corruption $p_{\mathbf{v}}$ ranging from 0 to 0.20, with fixed step-size 0.01.

The achieved results were evaluated by the commonly used objective criteria [39,41], such as the mean absolute error (MAE), the mean square error (MSE), and the normalized color difference (NCD). In designing the new filter class, we want to achieve the best balance between the noise suppression and color and edge information preservation and this balance will be documented using a variety of filtering results in forms of estimation errors and zoomed parts of the output images. Note that all tests were performed with the commonly used Euclidean norm ($\gamma = 2$) and a 3×3 filtering window.

The methods were tested using three test images Lena (Fig. 6A), Peppers (Fig. 6B), and Parrots (Fig. 6C) corrupted by a wide range of impulsive noise (Figs. 6D–F). Fig. 7 shows the output images and corresponding

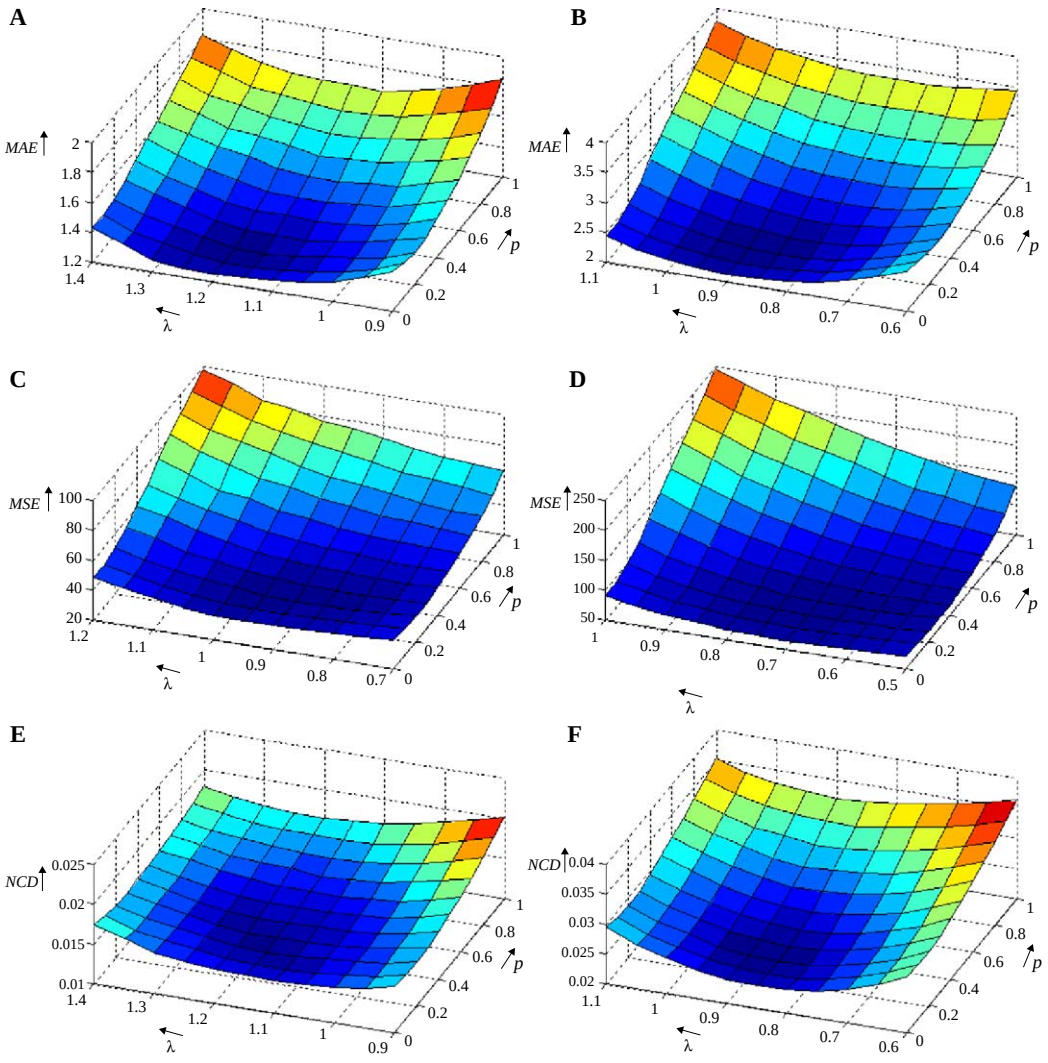

Fig. 10. Performance of the mean-based ASDDF in dependence on power parameter p and tuning parameter λ using the test image Lena corrupted by impulsive noise: (A, C, and E) $p_{\mathbf{v}} = 0.10$, (B, D, and F) $p_{\mathbf{v}} = 0.20$.

estimation errors achieved by applying the SVMF technique to the test image Lena corrupted by impulsive noise with $p_{\mathbf{v}} = 0.10$ (Fig. 6E) for the tuning parameter $\lambda = 0.1$ (Figs. 7A and D), $\lambda = 1$ (Figs. 7B and E), and $\lambda = 10$ (Figs. 7C and F). It can be seen easily that the SVMF preserves the details with the increased parameter λ. On the other hand, the excellent smoothing capability is achieved for smaller values of λ. Note that the SVMF filter provides the maximum amount of the smoothing for $\lambda = 0$, i.e., under the equivalence with the robust VMF. The smoothing capability of the SVMF filter gets worsen with the parameter λ, and for $\lambda > 10$ the proposed method practically preserves all data appearing in the filter input including outliers.

Figs. 8–11 evaluate the performance of the SDDF filter using objective measures MAE, MSE, and NCD in the dependence on the generalization parameter p and the tuning parameter λ. In this experiment, the test image Lena corrupted by impulsive noise $p_{\mathbf{v}} = 0.10$ (Fig. 6E) and $p_{\mathbf{v}} = 0.20$ (Fig. 6F) was used as the training set. As it can be seen, the sub-optimal value of λ decreases with the degree of the noise corruption. To perform another series of experiments presented in the sequence, accordingly to the results shown in Figs. 8–11 we selected the tuning parameter $\lambda = 4$ for the rank SDDFs, $\lambda = 12$ for the mean SDDFs, and also $\lambda = 1$ (i.e., no parameter) for both ASDDF schemes as the compromise for the considered degree of the impulsive noise corruption.

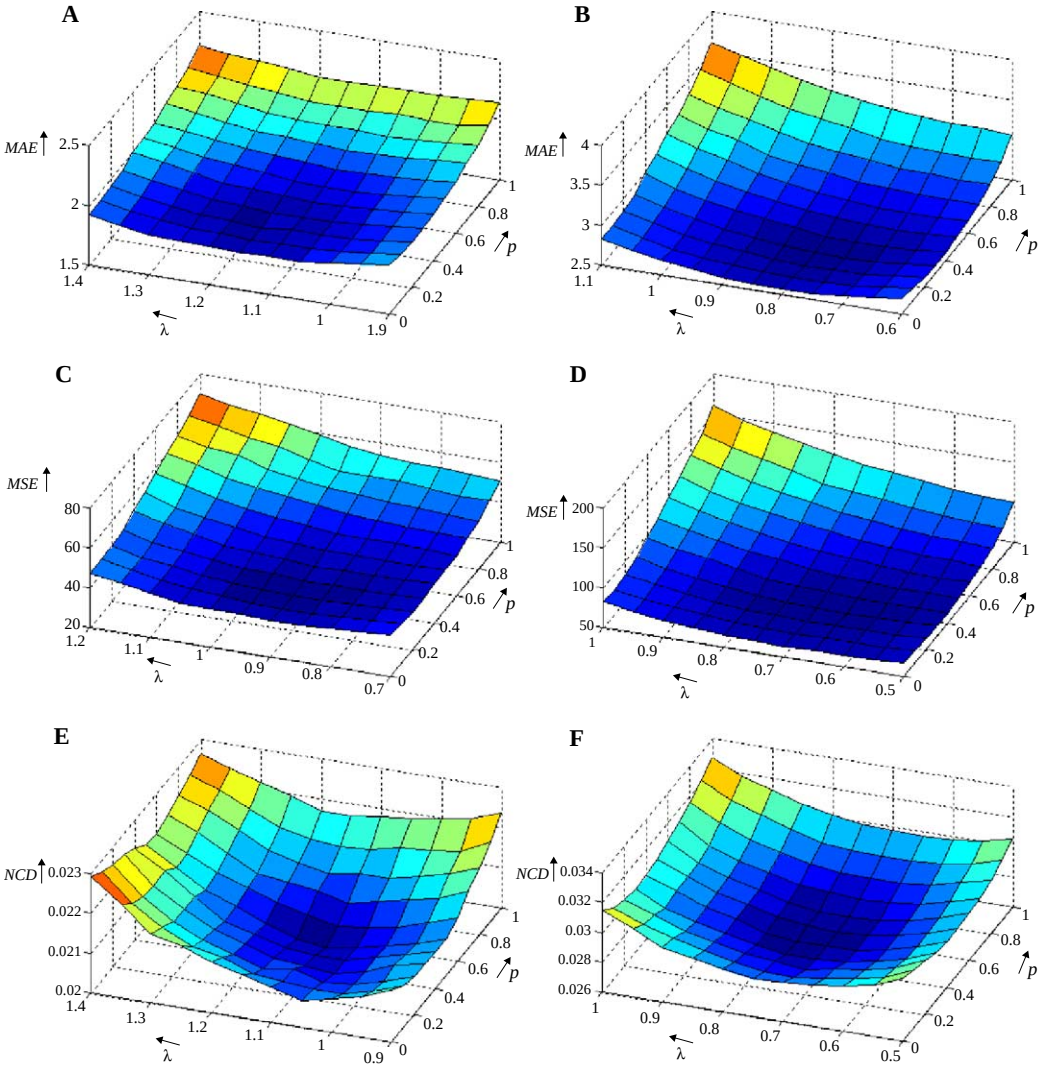

Fig. 11. Performance of the ranking-based ASDDF in dependence on power parameter p and tuning parameter λ using the test image Lena corrupted by impulsive noise: (A, C, and E) $p_{\mathbf{v}} = 0.10$, (B, D, and F) $p_{\mathbf{v}} = 0.20$.

Figs. 12–14 compare the performance of the ranking-based vector sigma filters (SDDF covering the SVMF and SBVDF as the special cases) and the mean-based adaptive vector sigma filters (ASDDF covering the ASVMF and ASBVDF as the special cases). In these experiments, we used all test images (Figs. 6A–C) and the results are achieved for the generalization parameter p ranging from 0 to 1 with step-size 0.1 and the impulsive noise intensity p_v ranging from 0 to 0.20 with step-size 0.01. These results show that the performance of the SDDF filter is similar for the whole range of the parameter p, although this technique achieves the best results for the power parameter p ranging from 0 to 0.5. In the case of ASDDF technique, the results are being changed more dramatically, especially for $p > 0.6$ when the filter fails to detect noisy pixels. The worst performance is visible for the noise intensities $p_v > 0.10$, especially in terms of the MSE criteria (Figs. 12D, 13D, and 14D). This shows that the noise suppression capability of the ASDDF filter is not sufficient

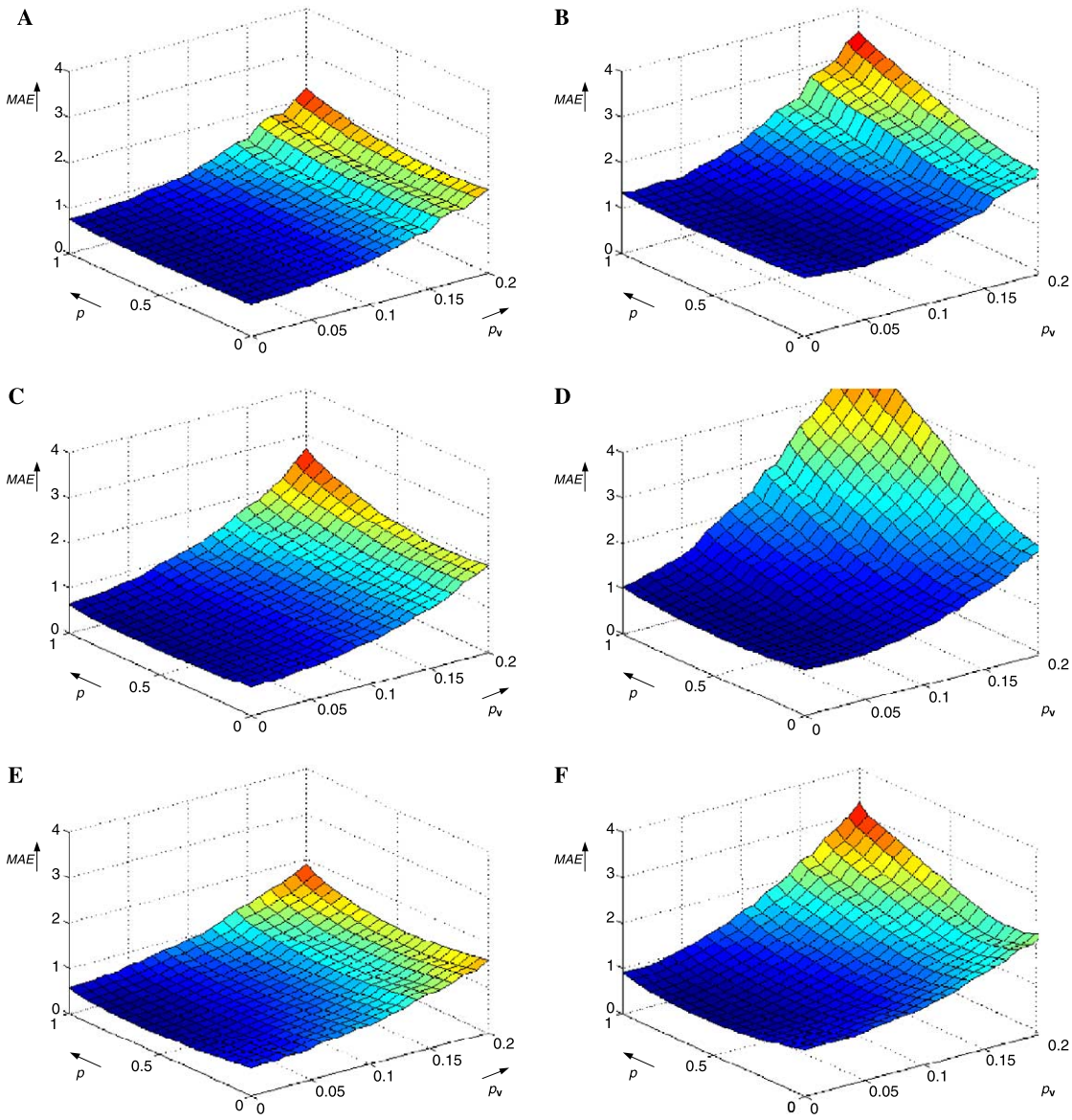

Fig. 12. Performance of rank SDDF (A, C, and E) and mean ASDDF (B, D, and F) methods expressed through MAE criteria in dependence on impulsive noise probability p_v and power parameter p: (A and B) test image Lena, (C and D) test image Peppers, and (E and F) test image Parrots.

for larger value of p, and the filter cannot be used for the noise suppression in highly corrupted images. For that reason it is not surprising that the best performance of the ASDDF filter is related to the smallest value of the power parameter p, which corresponds to the ASVMF technique. In addition to these results, the ASVMF represents the most computationally attractive case of the ASDDF method.

Finally, Figs. 15–17 show the zoomed parts of selected filtering techniques and Tables 1–3 summarize the achieved objective results. The performance of the proposed vector sigma filters (SVMF, SBVDF, and SDDF) and adaptive vector sigma filters (ASVMF, ASBVDF, and ASDDF) is compared with a variety of standard and adaptive filtering techniques such as componentwise median filter (MF) [18], adaptive switching medians based on local contrast probability (LCP) [31], and standard deviation-based scalar sigma filter (SF) [32]. These componentwise methods were compared with traditional vector filtering schemes such as previously described VMF [19], BVDF [21], DDF [43], GVDF [21], and vector hybrid filter (VHF) [42] and also recently

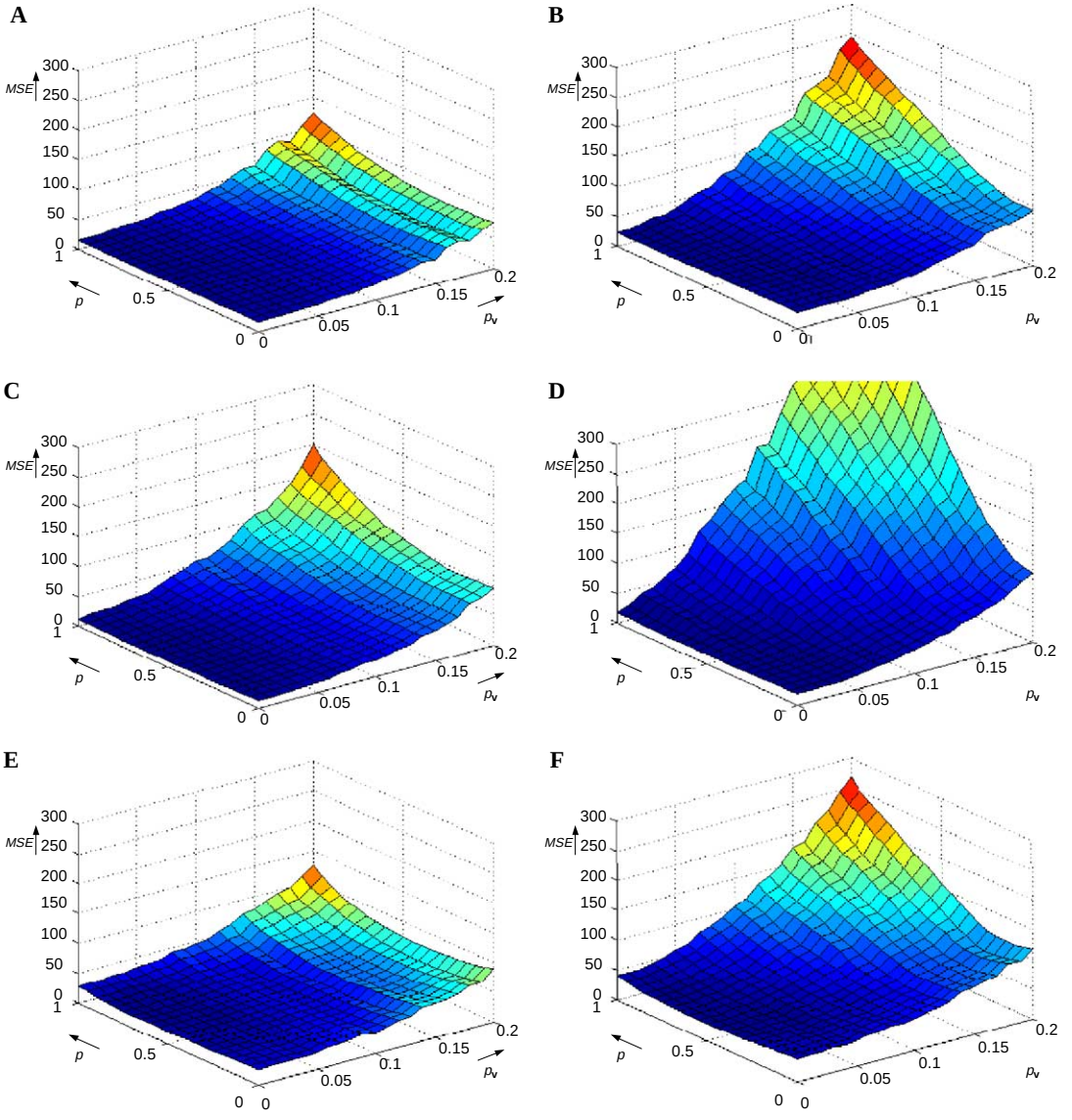

Fig. 13. Performance of rank SDDF (A, C, and E) and mean ASDDF (B, D, and F) methods expressed through MSE criteria in dependence on impulsive noise probability p_v and power parameter p: (A and B) test image Lena, (C and D) test image Peppers, and (E and F) test image Parrots.

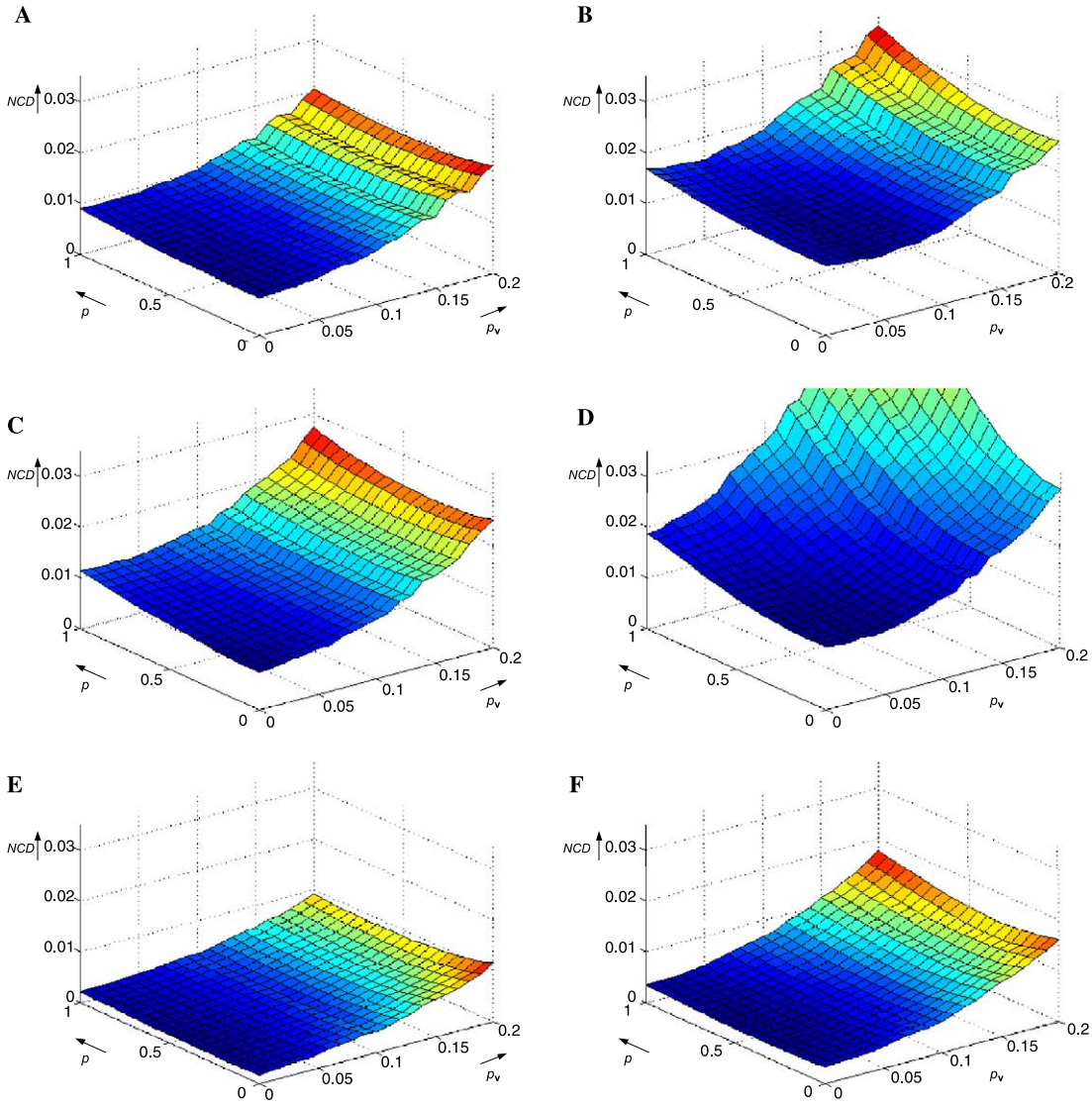

Fig. 14. Performance of rank SDDF (A, C, and E) and mean ASDDF (B, D, and F) methods expressed through NCD criteria in dependence on impulsive noise probability p_v and power parameter p: (A and B) test image Lena, (C and D) test image Peppers, and (E and F) test image Parrots.

introduced switching-based vector filters such as adaptive BVDF (ABVDF) [46], modified vector median (MVM) [58], and fuzzy adaptive vector directional filter (AVDF) [40]. Visual inspection of the zoomed images in Figs. 15–17 reveals that the standard filters excellently suppress impulses present in the image, however, some edges and image details are heavily blurred, especially at transitions between image regions. The use of adaptive methods significantly improves their signal-detail preserving capability and blurring can be significantly reduced. Since the color image denoising is a multi-criteria task, achieving the balance between noise smoothing and color/structural information preservation is of great importance in filter design.

If the proposed methods are compared with the adaptive algorithms such as componentwise LCP and SF or efficient multichannel techniques such as ABVDF, MVM, and AVDF, then these comparisons also show that the proposed method is clearly superior and outperforms the presented standard and adaptive filtering techniques in terms of objective quality measures (Tables 1–3). The proposed method is more robust in comparison with ABVDF technique, which provides excellent results for lowly corrupted images whereas its smoothing capability fails with increased impulsive noise corruption. Moreover, the proposed method is char-

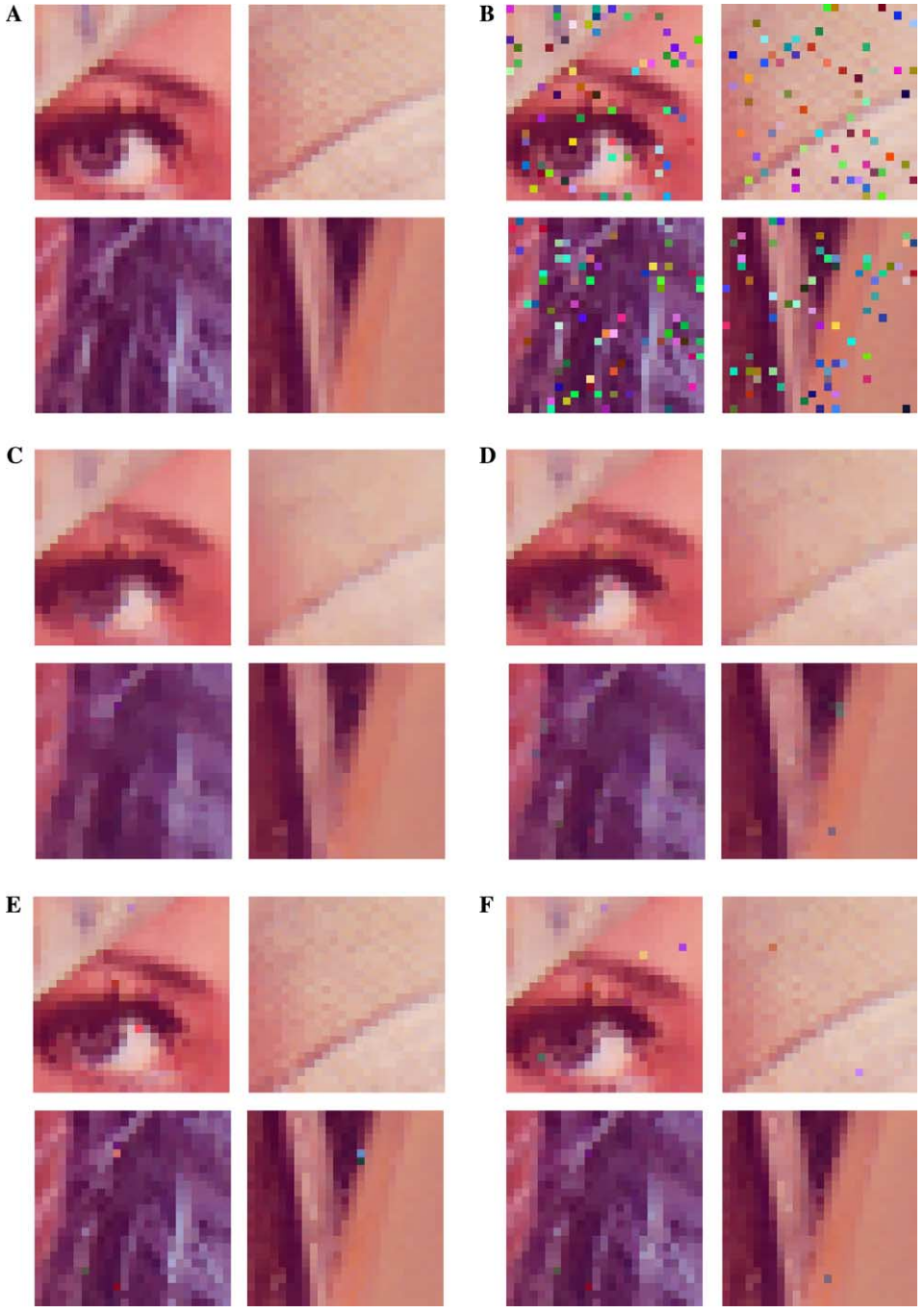

Fig. 15. Zoomed parts of test images and achieved results related to the test image Lena. (A) original image Lena, (B) test image Lena corrupted by impulsive noise $p_v = 0.10$, (C) VMF, (D) LCP approach, (E) proposed rank SVMF, and (F) proposed mean ASVMF.

acterized by significantly improved preservation capability in comparison with the MVM method. In addition, the proposed SVMF and ASVMF filters are able to remove the noise sufficiently, although there can be observed some situations when the local statistical properties of the corrupted image prevent removing all the outliers. Therefore, it can be claimed that the filters designed within the proposed framework achieve the best balance between the noise suppression and the signal-detail preservation among the tested methods.

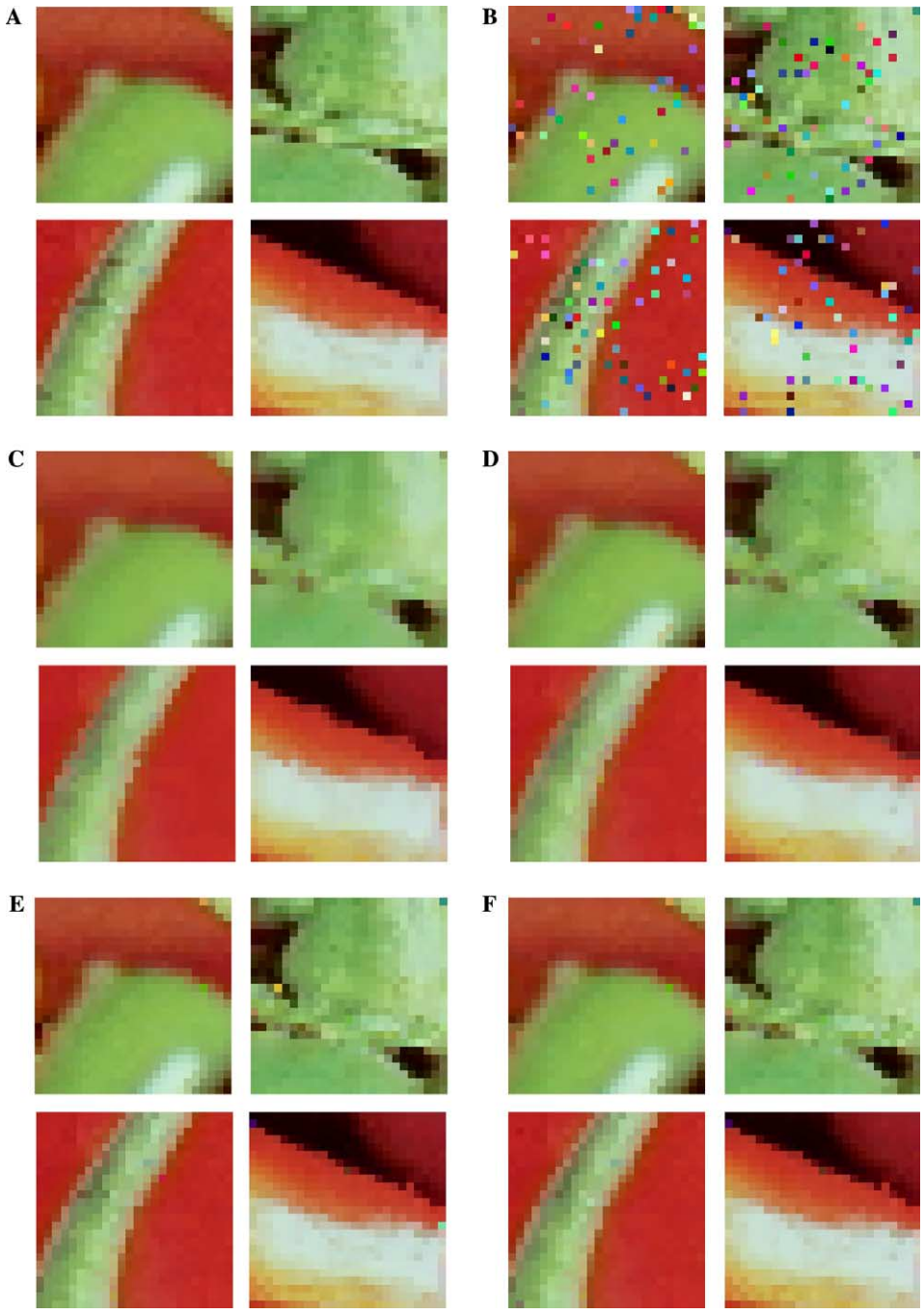

Fig. 16. Zoomed parts of test images and achieved results related to the test image Peppers. (A) Original image Peppers, (B) test image Peppers corrupted by impulsive noise $p_v = 0.10$, (C) VMF, (D) LCP approach, (E) proposed rank SVMF, and (F) proposed mean ASVMF.

5. Conclusion

In this paper, a new color image filtering framework has been proposed. The framework is based on order-statistic theory and statistical switching using standard deviation or approximation of the variance both computed

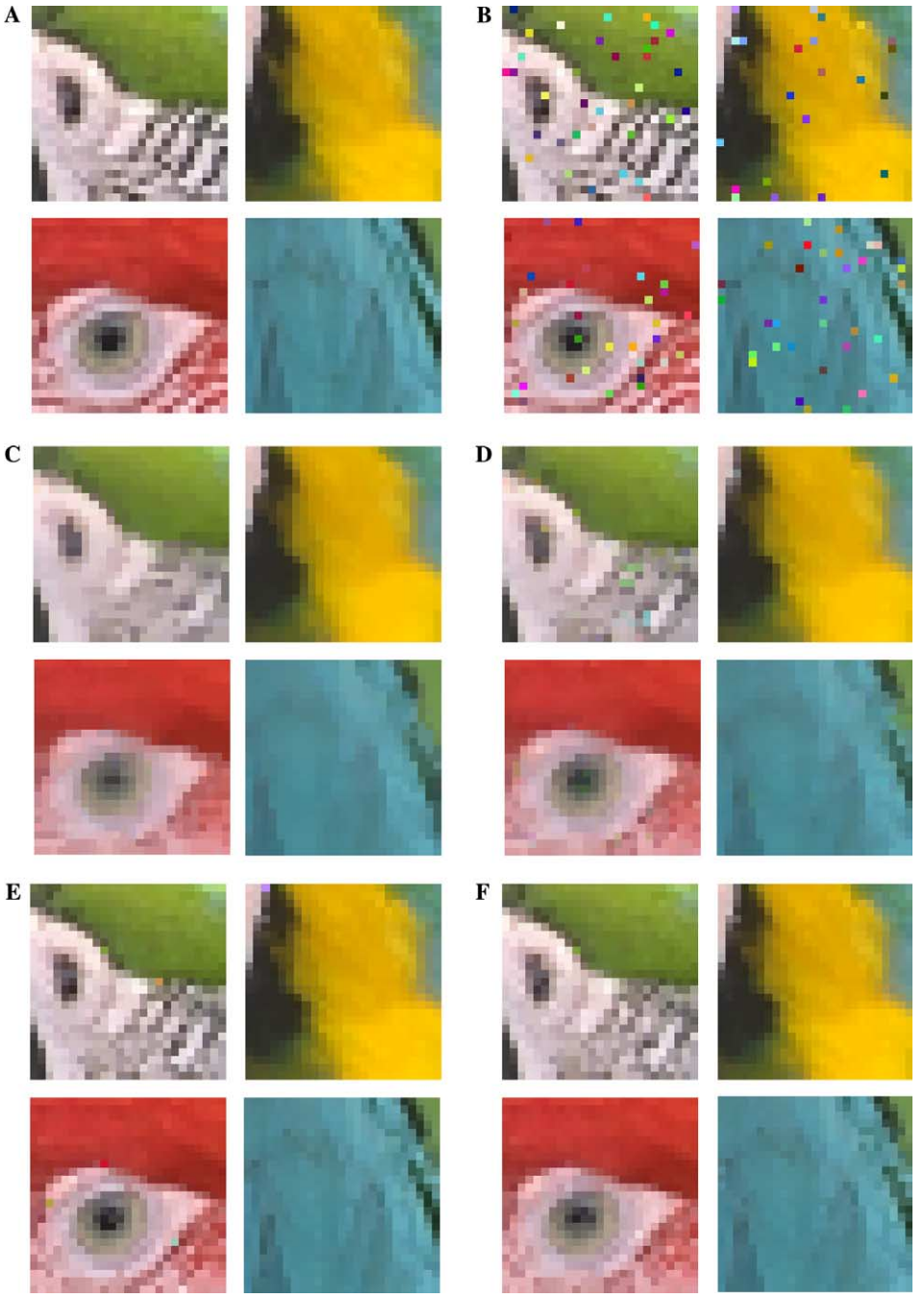

Fig. 17. Zoomed parts of test images and achieved results related to the test image Parrots. (A) Original image Parrots, (B) test image Parrots corrupted by impulsive noise $p_v = 0.05$, (C) VMF, (D) LCP approach, (E) proposed rank SVMF, and (F) proposed mean ASVMF.

using the input samples spawned by a filtering window. The achieved results show excellent detection and signal-detail preservation capabilities of the new approach, while still holding the impulsive noise attenuation characteristics of standard vector filters. The new filters clearly outperform the standard vector filtering schemes as well as their adaptive modifications. In our experiments, the best results were achieved by sigma VMF and adaptive sigma VMF schemes that are the most computationally attractive cases of the proposed filter class.

Table 1
Comparison of the presented algorithms using impulsive noise corruption $p_v = 0.05$

Image	Lena			Peppers			Parrots		
Method/criterion	MAE	MSE	NCD	MAE	MSE	NCD	MAE	MSE	NCD
Noisy	3.762	427.3	0.0445	3.988	486.1	0.0441	3.805	443.6	0.0432
MF	3.394	49.7	0.0442	3.248	43.1	0.0484	2.718	63.1	0.0170
VMF	3.430	50.8	0.0403	3.169	43.9	0.0452	2.669	64.2	0.0132
BVDF	3.818	58.6	0.0407	3.740	60.7	0.0438	3.460	109.0	0.0116
DDF	3.509	52.3	0.0402	3.182	44.6	0.0431	2.645	65.3	0.0117
AVDF	4.301	54.3	0.0483	4.068	51.4	0.0552	3.802	94.5	0.0147
GVDF	3.587	55.3	0.0420	3.433	57.9	0.0453	3.036	93.6	0.0126
HVF	3.857	56.9	0.0434	3.282	42.9	0.0441	2.786	65.7	0.0122
SF	1.764	33.3	0.0204	1.614	27.7	0.0217	1.416	45.5	0.0067
LCP	2.214	38.8	0.0263	2.046	33.1	0.0279	1.747	51.4	0.0086
MVM	1.312	30.1	0.0158	1.205	23.9	0.0144	1.185	41.1	0.0059
ABVDF	0.506	20.7	0.0044	0.610	26.1	0.0065	0.521	32.2	0.0017
Rank SVMF	0.777	18.3	0.0082	0.729	16.5	0.0090	0.699	27.8	0.0027
Mean SVMF	0.980	21.4	0.0103	0.878	18.2	0.0107	0.840	31.1	0.0031
Rank ASVMF	1.540	30.2	0.0174	1.410	27.9	0.0177	1.261	42.3	0.0058
Mean ASVMF	1.192	27.3	0.0127	1.033	23.0	0.0124	1.081	41.8	0.0040
Rank SBVDF	0.805	19.1	0.0089	0.789	22.7	0.0113	0.694	34.3	0.0026
Mean SBVDF	1.054	27.6	0.0115	0.987	34.4	0.0129	0.875	44.8	0.0032
Rank ASBVDF	1.717	40.6	0.0182	1.603	40.1	0.0193	1.464	60.7	0.0054
Mean ASBVDF	1.313	37.6	0.0155	1.391	65.9	0.0219	1.056	57.7	0.0043
Rank SDDF	0.731	16.4	0.0080	0.649	14.6	0.0096	0.545	21.2	0.0024
Mean SDDF	0.948	19.9	0.0105	0.816	17.9	0.0111	0.678	25.9	0.0027
Rank ASDDF	1.537	31.6	0.0171	1.352	28.9	0.0172	1.133	38.8	0.0049
Mean ASDDF	1.153	28.2	0.0131	1.004	31.1	0.0140	0.783	32.2	0.0033

Table 2
Comparison of the presented algorithms using impulsive noise corruption $p_v = 0.10$

Image	Lena			Peppers			Parrots		
Method/criterion	MAE	MSE	NCD	MAE	MSE	NCD	MAE	MSE	NCD
Noisy	7.312	832.0	0.0840	7.677	943.3	0.0869	7.526	882.0	0.0857
MF	3.703	56.8	0.0489	3.579	53.9	0.0546	2.960	70.0	0.0198
VMF	3.687	56.5	0.0428	3.503	55.0	0.0494	2.890	69.6	0.0142
BVDF	4.099	67.6	0.0432	4.151	82.7	0.0484	3.630	113.5	0.0127
DDF	3.733	57.3	0.0424	3.512	56.6	0.0475	2.839	69.7	0.0128
AVDF	4.540	59.5	0.0503	4.370	61.6	0.0592	3.984	98.1	0.0155
GVDF	3.925	66.8	0.0448	3.785	73.4	0.0492	3.188	96.2	0.0137
HVF	3.857	56.9	0.0434	3.626	53.6	0.0486	3.002	69.9	0.0132
SF	1.775	37.1	0.0207	1.667	36.2	0.0225	1.507	51.6	0.0078
LCP	2.254	43.1	0.0271	2.101	41.6	0.0288	1.824	57.3	0.0095
MVM	1.453	31.3	0.0152	1.279	28.6	0.0151	1.362	45.2	0.0063
ABVDF	0.936	38.6	0.0080	1.195	56.9	0.0143	1.031	68.2	0.0033
Rank SVMF	0.959	25.9	0.0105	0.941	27.4	0.0117	0.862	35.4	0.0041
Mean SVMF	1.123	28.3	0.0121	1.063	29.0	0.0133	1.016	40.6	0.0047
Rank ASVMF	1.883	38.7	0.0210	1.768	39.8	0.0225	1.589	52.6	0.0075
Mean ASVMF	1.332	36.2	0.0144	1.265	39.9	0.0158	1.252	52.6	0.0060
Rank SBVDF	1.048	33.1	0.0105	1.155	56.7	0.0135	0.941	47.4	0.0035
Mean SBVDF	1.311	48.6	0.0131	1.533	99.1	0.0174	1.129	67.1	0.0045
Rank ASBVDF	2.132	55.6	0.022	2.144	75.7	0.0239	1.929	91.9	0.0072
Mean ASBVDF	1.721	76.3	0.0182	2.239	173.4	0.0305	1.569	105.0	0.0067
Rank SDDF	0.913	23.3	0.0098	0.895	30.2	0.0117	0.703	25.9	0.0030
Mean SDDF	1.094	28.3	0.0118	1.103	44.0	0.0142	0.843	33.5	0.0037
Rank ASDDF	1.886	40.9	0.0207	1.781	48.0	0.0221	1.448	50.9	0.0064
Mean ASDDF	1.378	46.7	0.0147	1.514	84.6	0.0191	1.106	56.6	0.0052

Table 3
Comparison of the presented algorithms using impulsive noise corruption $p_v = 0.20$

Image	Lena			Peppers			Parrots		
Method/criterion	MAE	MSE	NCD	MAE	MSE	NCD	MAE	MSE	NCD
Noisy	14.019	1604.6	0.1625	14.912	1832.0	0.1694	14.213	1663.0	0.1608
MF	4.521	87.9	0.0619	4.487	91.4	0.0726	3.623	97.3	0.0276
VMF	4.335	80.3	0.0492	4.232	85.7	0.0601	3.448	91.9	0.0174
BVDF	4.859	107.8	0.0499	5.111	152.9	0.0602	4.183	140.0	0.0165
DDF	4.321	78.8	0.0483	4.254	90.4	0.0579	3.386	91.2	0.0161
AVDF	5.258	80.4	0.0572	5.226	98.3	0.0739	4.016	118.1	0.0175
GVDF	4.345	83.4	0.0493	4.562	122.4	0.0586	3.450	100.9	0.0174
HVF	4.548	80.4	0.0500	4.411	86.4	0.0599	3.594	92.7	0.0169
SF	2.295	66.5	0.0284	2.267	73.6	0.0326	2.036	83.4	0.0136
LCP	2.739	70.6	0.0345	2.743	79.5	0.0404	2.290	85.0	0.0148
MVM	1.847	52.5	0.0198	1.785	57.2	0.0226	1.537	73.5	0.0102
ABVDF	1.974	90.4	0.0170	2.502	142.7	0.0277	1.952	129.5	0.0072
Rank SVMF	1.816	77.6	0.0212	1.898	97.3	0.0251	1.618	90.0	0.0116
Mean SVMF	1.928	75.4	0.0221	1.995	94.2	0.0266	1.803	96.3	0.0128
Rank ASVMF	2.629	75.2	0.0303	2.550	83.5	0.0340	2.262	89.0	0.0142
Mean ASVMF	2.221	91.7	0.0260	2.333	115.4	0.0310	2.183	117.0	0.0161
Rank SBVDF	2.232	122.9	0.0203	2.676	199.8	0.0275	1.907	126.3	0.0092
Mean SBVDF	2.708	171.0	0.0245	3.638	332.1	0.0385	2.568	196.1	0.0128
Rank ASBVDF	3.300	145.7	0.0316	3.495	190.6	0.0365	3.084	188.7	0.0139
Mean ASBVDF	3.501	245.2	0.0327	5.118	501.5	0.0631	3.253	269.2	0.0177
Rank SDDF	1.803	77.5	0.0192	1.953	109.9	0.0239	1.417	74.9	0.0087
Mean SDDF	2.034	91.3	0.0212	2.389	151.6	0.0289	1.672	91.6	0.0101
Rank ASDDF	2.748	92.6	0.0293	2.748	112.2	0.0329	2.212	99.2	0.0118
Mean ASDDF	2.658	150.0	0.0268	3.499	287.6	0.0415	2.329	156.8	0.0145

References

[1] R. Lukac, B. Smolka, K. Martin, K.N. Plataniotis, A.N. Venetsanopoulos, Vector filtering for color imaging, IEEE Signal Process. Mag., Special Issue on Color Image Processing 22 (2005) 74–86.
[2] K.N. Plataniotis, A.N. Venetsanopoulos, Color Image Processing and Applications, Springer Verlag, Berlin, 2000.
[3] I. Pitas, P. Tsakalides, Multivariate ordering in color image filtering, IEEE Trans. Circuits Syst. Video Technol. 1 (1991) 247–259.
[4] B. Smolka, A. Chydzinski, K. Wojciechowski, K.N. Plataniotis, A.N. Venetsanopoulos, On the reduction of impulsive noise in multichannel image processing, Opt. Eng. 40 (2001) 902–908.
[5] J. Astola, P. Kuosmanen, Fundamentals of Nonlinear Digital Filtering, CRC Press, Boca Raton, FL, 1997.
[6] S. Peltonen, M. Gabbouj, J. Astola, Nonlinear filter design: methodologies and challenges, in: Proceedings of the IEEE Region 8-EURASIP Symposium on Image and Signal Processing and Analysis ISPA'01 in Pula, Croatia, 2001, pp. 102–106.
[7] I. Pitas, A.N. Venetsanopoulos, Nonlinear Digital Filters, Principles and Applications, Kluwer Academic Publishers, Dordrecht, 1990.
[8] R. Lukac, K.N. Plataniotis, B. Smolka, A.N. Venetsanopoulos, A multichannel order-statistic technique for cDNA microarray image processing, IEEE Trans. Nanobiosci. 3 (2004) 272–285.
[9] R. Lukac, K.N. Plataniotis, B. Smolka, A.N. Venetsanopoulos, cDNA microarray image processing using fuzzy vector filtering framework, J. Fuzzy Sets Syst., Special Issue on Fuzzy Sets and Systems in Bioinformatics 152 (2005) 17–35.
[10] M. Barni, F. Bartolini, V. Capellini, Image processing for virtual restoration of artworks, IEEE Multimedia (2000) 34–37.
[11] X. Li, D. Lu, Y. Pan, Color restoration and image retrieval for Donhunag fresco preservation, IEEE Multimedia (2000) 38–42.
[12] A. Kokaram, Motion Picture Restoration, Springer-Verlag, Berlin, 1998.
[13] L. Tenze, S. Carrato, G. Ramponi, An alignment algorithm for old motion pictures, IEEE Signal Process. Lett. 9 (2002) 309–311.
[14] <www.foto.unibas.ch/research/paper3/filmrest.html/>. Restoration of old movie films by digital image processing, visited December 2002.
[15] N.J. Garber, L.A. Hoel, Traffic and Highway Engineering, Brooks/Cole Publishing, Pacific Grove, CA, 1999.
[16] <www.imagesensing.com/>. Image sensing systems incorporated, visited January 2000.
[17] H. Rantanen, M. Karlsson, P. Pohjala, S. Kalli, Color video signal processing with median filters, IEEE Trans. Consum. Electr. 38 (1992) 157–161.
[18] J. Zheng, K.P. Valavanis, J.M. Gauch, Noise removal from color images, J. Intell. Robot. Syst. 7 (1993) 257–285.
[19] J. Astola, P. Haavisto, Y. Neuvo, Vector median filters, Proc. IEEE 78 (1990) 678–689.

[20] R. Lukac, Adaptive vector median filtering, Pattern Recogn. Lett. 24 (2003) 1889–1899.
[21] P.E. Trahanias, D. Karakos, A.N. Venetsanopoulos, Directional processing of color images: theory and experimental results, IEEE Trans. Image Process. 5 (1996) 868–881.
[22] K.N. Plataniotis, D. Androutsos, A.N. Venetsanopoulos, Adaptive fuzzy systems for multichannel signal processing, Proc. IEEE 87 (1999) 1601–1622.
[23] I. Pitas, A.N. Venetsanopoulos, Order statistics in digital image processing, Proc. IEEE 80 (1992) 1892–1919.
[24] S. Mitra, J. Sicuranza, Nonlinear Image Processing, Academic Press, New York, 2001.
[25] R. Lukac, B. Smolka, K.N. Plataniotis, A.N. Venetsanopulos, Selection weighted vector directional filters, Comput. Vision Image Understand., Special Issue on Colour for Image Indexing and Retrieval 94 (2004) 140–167.
[26] L. Lucat, P. Siohan, D. Barba, Adaptive and global optimization methods for weighted vector median filters, Signal Process.: Image Commun. 17 (2002) 509–524.
[27] T. Viero, K. Oistamo, Y. Neuvo, Three-dimensional median related filters for color image sequence filtering, IEEE Trans. Circuits Syst. Video Technol. 4 (1994) 129–142.
[28] Y. Hashimoto, Y. Kajikawa, Y. Nomura, Directional difference-based switching median filters, Electron. Commun. Japan 85 (Part 3) (2002) 22–32.
[29] Y. Hashimoto, Y. Kajikawa, Y. Nomura, Directional difference filters: its effectiveness in the postprocessing of noise detectors, Electron. Commun. Japan 85 (Part 3) (2002) 74–82.
[30] M. Szczepanski, B. Smolka, K.N. Plataniotis, A.N. Venetsanopoulos, On the geodesic paths approach to color image filtering, Signal Process. 83 (2003) 1309–1342.
[31] A. Beghdadi, K. Khellaf, A noise-filtering method using a local information measure, IEEE Trans. Image Process. 6 (1997) 879–882.
[32] J.S. Lee, Digital image smoothing and the sigma filter, Computer Vision Graph. Image Process. 24 (1983) 255–269.
[33] T. Chen, H.R. Wu, Adaptive impulse detection using center-weighted median filters, IEEE Signal Process. Lett. 8 (2001) 1–3.
[34] H.L. Eng, K.K. Ma, Noise adaptive soft-switching median filter, IEEE Trans. Image Process. 10 (2001) 242–251.
[35] S. Zhang, M.A. Karim, A new impulse detector for switching median filters, IEEE Signal Process. Lett. 9 (2002) 360–363.
[36] K. Tang, J. Astola, Y. Neuvo, Nonlinear multivariate image filtering techniques, IEEE Trans. Image Process. 4 (1995) 788–798.
[37] B. Smolka, R. Lukac, A. Chydzinski, K.N. Plataniotis, K. Wojciechowski, Fast adaptive similarity based impulsive noise reduction filter, Real-Time Imaging, Special Issue on Spectral Imaging 9 (2003) 261–276.
[38] A.J. Bardos, S.J. Sangwine, Selective vector median filtering of colour images, in: Proceedings of the 6th International Conference on Image Processing and its Applications, vol. 2, 1997, pp. 708–711.
[39] R. Lukac, Adaptive color image filtering based on center-weighted vector directional filters, Multidim. Syst. Signal Process. 15 (2004) 169–196.
[40] K.N. Plataniotis, D. Androutsos, A.N. Venetsanopoulos, Color image processing using adaptive vector directional filters, IEEE Trans. Circuits Syst. II 45 (1998) 1414–1419.
[41] R. Lukac, K.N. Plataniotis, B. Smolka, A.N. Venetsanopoulos, Generalized selection weighted vector filters, EURASIP J. Appl. Signal Process., Special Issue on Nonlinear Signal and Image Processing—Part I 2004 (2004) 1870–1885.
[42] M. Gabbouj, A. Cheickh, Vector median-vector directional hybrid filter for color image restoration, in: Proceedings of the European Signal Processing Conference (EUSIPCO), 1996, pp. 879–881.
[43] D.G. Karakos, P.E. Trahanias, Generalized multichannel image-filtering structure, IEEE Trans. Image Process. 6 (1997) 1038–1045.
[44] R.O. Duda, P.E. Hart, Pattern Classification and Scene Analysis, Wiley, New York, 1973.
[45] M. Barni, V. Cappelini, A. Mecocci, Fast vector median filter based on Euclidean norm approximation, IEEE Signal Process. Lett. 1 (1994) 92–94.
[46] R. Lukac, Color image filtering by vector directional order-statistics, Pattern Recogn. Image Anal. 12 (2002) 279–285.
[47] K.E. Barner, G.R. Arce, Design of permutation order statistic filters through group coloring, IEEE Trans. Circuit Syst. II 44 (1997) 531–547.
[48] B. Smolka, K.N. Plataniotis, A. Chydzinski, M. Szczepanski, A.N. Venetsanopulos, K. Wojciechowski, Self-adaptive algorithm of impulsive noise reduction in color images, Pattern Recogn. 35 (2002) 1771–1784.
[49] R. Lukac, B. Smolka, K.N. Plataniotis, Color sigma filter, in: Proceedings of the 9th International Workshop on Systems, Signals and Image Processing IWSSIP'02 in Manchester, UK, 2002, pp. 559–565.
[50] R. Lukac, B. Smolka, K.N. Plataniotis, A.N. Venetsanopoulos, P. Zavarsky, Angular multichannel sigma filter, in: Proceedings of the 28th IEEE International Conference on Acoustic, Speech and Signal Processing ICASSP 2003 in Hong-Kong, vol. III, 2003, pp. 745–748.
[51] R. Lukac, B. Smolka, K.N. Plataniotis, A.N. Venetsanopoulos, Generalized adaptive vector sigma filters, in: Proceedings of the IEEE International Conference on Multimedia and Expo (ICME 2003) in Baltimore, USA, vol. I, 2003, pp. 537–540.
[52] R. Lukac, K.N. Plataniotis, A.N. Venetsanopoulos, B. Smolka, A statistically-switched adaptive vector median filter, J. Intell. Robotic Syst. 42 (2005) 361–391.
[53] S.S. Wilks, Certain generalizations in the analysis of variance, Biometrika 24 (1932) 471–494.
[54] G.A.F. Seber, Multivariate Observations, Wiley, New York, 1984.
[55] T.W. Anderson, An Introduction to Multivariate Statistical Analysis, second ed., Wiley, New York, 1984.
[56] K.V. Mardia, J.T. Kent, J.M. Bibby, Multivariate Analysis, Academic Press, New York, 1979.
[57] S. Mustonen, A measure for total variability in multivariate normal distribution, Comput. Stat. Data Anal. 23 (1997) 321–334.
[58] B. Smolka, M.K. Szczepanski, K.N. Plataniotis, A.N. Venetsanopoulos, On the modified weighted vector median filter, in: Proceedings of Digital Signal Processing DSP'02, Santorini, Greece, vol. 2, 2002, pp. 939–942.